

Utah State University

DigitalCommons@USU

All Graduate Theses and Dissertations

Graduate Studies

5-2016

Structural Insights into the Regulation of Electron Transfer in Nitrogenase, and Modulating the Reactivity of the Isolated Iron Molybdenum Cofactor

Andrew J. Rasmussen
Utah State University

Follow this and additional works at: <https://digitalcommons.usu.edu/etd>

 Part of the [Other Chemistry Commons](#)

Recommended Citation

Rasmussen, Andrew J., "Structural Insights into the Regulation of Electron Transfer in Nitrogenase, and Modulating the Reactivity of the Isolated Iron Molybdenum Cofactor" (2016). *All Graduate Theses and Dissertations*. 4897.

<https://digitalcommons.usu.edu/etd/4897>

This Thesis is brought to you for free and open access by the Graduate Studies at DigitalCommons@USU. It has been accepted for inclusion in All Graduate Theses and Dissertations by an authorized administrator of DigitalCommons@USU. For more information, please contact digitalcommons@usu.edu.



STRUCTURAL INSIGHTS INTO THE REGULATION OF ELECTRON TRANSFER IN
NITROGENASE, AND MODULATING THE REACTIVITY OF
THE ISOLATED IRON MOLYBDENUM COFACTOR

by

Andrew J. Rasmussen

A thesis submitted in partial fulfillment
of the requirements for the degree

of

MASTER OF SCIENCE

in

Biochemistry

Approved:

Lance C. Seefeldt
Major Professor

Scott A. Ensign
Committee Member

Jeanette Norton
Committee Member

Mark McLellan
Vice President for Research and
Dean of Graduate Studies

UTAH STATE UNIVERSITY
Logan, Utah
2016

Copyright © Andrew J. Rasmussen 2015

All Right Reserved

ABSTRACT

STRUCTURAL INSIGHTS INTO THE REGULATION OF ELECTRON TRANSFER IN
NITROGENASE, AND MODULATING THE REACTIVITY OF
THE ISOLATED IRON MOLYBDENUM COFACTOR

by

Andrew J. Rasmussen, Master of Science

Utah State University, 2016

Major Professor: Dr. Lance C. Seefeldt
Department: Chemistry and Biochemistry

Nitrogenase, EC: [1.18.6.1](#) is the enzyme that catalyzes the reduction of dinitrogen to ammonia; this is known as biological nitrogen fixation. Nitrogen fixation is so important to our daily lives, that we utilize approximately 2% of the annual energy produced worldwide to fix nitrogen industrially via the Haber-Bosch process. The industrial process requires a high input of energy in the form of heat (>450° C) and pressure (>200 atm), while the enzymatic system is performed under ambient conditions. Research invested into understanding the mechanism of this biological catalyst could eventually lead to understanding how nature performs difficult chemical reductions, which could allow researchers to develop catalysts that mimic this enzyme to perform many important reactions, such as nitrogen fixation, much more efficiently than today.

Electron transfer in the nitrogenase is only partially understood, and is one of the key elements of understanding the mechanism of nitrogenase. Nitrogenase is composed of two proteins, the Fe protein delivers electrons to the MoFe protein, where N₂ binds and is

subsequently reduced. The conformational changes that take place upon Fe protein binding were investigated in order to better understand electron transfer within the enzyme. Further, studies were performed which probed the P-cluster, an iron sulfur cluster in the MoFe protein that acts as an intermediate in the electron transfer event, and successfully identified the biologically relevant redox state of the P-cluster, P^{+1} . Other studies were performed which identified several variants of the MoFe protein which were able to accept electrons from a chemical reductant. These variants are the first examples of nitrogenase enzymes able to accept electrons from any source other than Fe protein and shown substrate reduction. These variants pinpoint where nitrogenase is likely to undergo conformational changes to allow electron transfer to the active site of the enzyme. Finally, studies were done on the isolated active site of the protein, the iron molybdenum cofactor to better understand how the active site of nitrogenase works. The goal of this thesis is to better understand how electrons travel through nitrogenase, and how they are utilized at the active site, FeMo-cofactor, when they arrive.

(102 pages)

PUBLIC ABSTRACT

STRUCTURAL INSIGHTS INTO THE REGULATION OF ELECTRON TRANSFER IN
NITROGENASE, AND MODULATING THE REACTIVITY OF
THE ISOLATED IRON MOLYBDENUM COFACTOR

Andrew J. Rasmussen

One of the most important scientific advances in the last century was the Haber-Bosch process, the industrial process of fixing nitrogen from the atmosphere to ammonia. This allowed for the commercial production and sale of nitrogen for important uses such as fertilizer for farming. The Haber-Bosch process is partially credited with the population boom that has been seen in the last century and has greatly increased the standard of living in the developed world today. While this was a great scientific breakthrough, the cost of producing the required ammonia is high, and roughly 2% of worldwide energy is used annually to meet this demand. There are many microorganisms that can produce ammonia, known as diazotrophs, and indeed roughly half of all ammonia produced annually is produced by these microorganisms. Diazotrophs can fix nitrogen much more efficiently than our industrial process today, and research is being done to better understand the mechanism of biological nitrogen reduction.

The enzyme responsible for nitrogen fixation is known as nitrogenase, and has two component proteins. The MoFe protein is the catalytic enzyme and the Fe protein is the source of the electrons which provide the energy to reduce nitrogen. One of the key questions in nitrogenase catalysis is how the electrons that are provided by the Fe protein are transferred into and utilized by the MoFe protein to reduce nitrogen and produce ammonia.

The goal of this thesis is to better understand how electrons travel through nitrogenase, and how they are utilized at the active site, FeMo-cofactor, when they arrive.

ACKNOWLEDGMENTS

I would be remiss if I didn't first acknowledge my family and loved ones for supporting me a teaching how to live, which allowed me to get to this point in my life. I would like to thank my mother and father for raising me to work hard and to value knowledge, my sisters for teaching me how to work with others and to have fun while doing so. They have encouraged me through all my choices even when they saw that I was not taking the easiest path toward my goals, and they have rejoiced with my successes, and helped me through my failures. I would also like to thank my wife who has stood by me for the last seven years, even when she thought I was crazy for attempting graduate school. She has supported me and encouraged me to strive for the best in myself. Summer your love and support has meant everything to me, and I would not be where I am today without you. I am grateful to God for the gift of a wonderful family, a sound mind, and a healthy body, all of which have allowed me to pursue a career in science that has been fulfilling and enjoyable.

Further, those I work with on a daily basis deserve much credit for what I have achieved over the last three years. First there was Dr Lance Seefeldt, who came and gave a presentation to the senior undergraduates at Weber state university. He first sparked an interest in the world of research and planted the seed of attending graduate school in my mind. Second there was Dr. Andrew Lippert, who helped me to develop a love of chemistry when I was simply taking the classes necessary to earn a degree. He loved teaching and he was able to connect with me in a way few other professors have ever been able to repeat. Next, to all of my committee members who have had to deal with my procrastination and missing my deadlines for submitting my work, thank you for the patience and encouragement you always showed to me, even when I know you must have been frustrated.

I would like to thank the friends I have made in the department, who were great examples and colleagues. Foremost of these would be Danyal, who took me under his wing and taught me what to do and how to act to be successful in a graduate lab. Also, Nimesh and Sudipto, you were both great friends and helped me to mature into a better scientist by simply being around me. I learned something new every time I spoke with you. Derek and Rhesa, you also were influential in my time in the lab. You both work so hard and were great examples to me of dedication to the science. I hope to become as good a scientist as you all already are. Thank you for being great friends.

There are a great many more that deserve my thanks for making USU a wonderful place to perform research, and I am thankful to everyone in the department.

Andrew J. Rasmussen

CONTENTS

	Page
ABSTRACT	iii
PUBLIC ABSTRACT	v
ACKNOWLEDGMENTS	vii
CONTENTS	ix
LIST OF TABLES	xi
LIST OF FIGURES	xii
LIST OF EQUATIONS	xiv
ABBREVIATIONS	xv
CHAPTER	
I. INTRODUCTION	1
Abstract	1
Significance.....	1
Interactions of MoFe and Fe Proteins: The Fe Cycle	4
The Metal Clusters of Nitrogenase	6
Electron Transfer in Nitrogenase	10
Summary	11
References.....	13
II. CONFORMATIONAL GATING OF THE ATP HYDROLYSIS AND PHOSPHATE RELEASE STEPS OF THE Fe CYCLE	15
Abstract	15
Experimental Procedures	16
Results and Discussions	18
Conclusions.....	19
References.....	22
III. ELECTROCHEMICALLY POISING THE P CLUSTER OF NITROGENASE AT DEFINED POTENTIALS: CAPTURING THE STRUCTURE OF AN ELECTRON TRANSFER INTERMEDIATE	23
Abstract	23
Experimental Procedure.....	25
Results and Discussions	28
Acknowledgments.....	31
References.....	36

IV. Fe PROTEIN-INDEPENDANT SUBSTRATE REDUCTION BY NITROGENASE MoFe PROTEIN VARIANTS	37
Abstract	37
Experimental Procedures	41
Results and Discussions	45
Structural Characterization	49
Calculations on Normal-Mode Conformational Changes.....	51
Conclusions	54
References	56
Supporting Information.....	60
 V. CHARACTERIZATION AND MODULATION OF THE ISOLATED IRON MOLYBDENUM COFACTOR	64
Abstract	64
Experimental Procedures	66
Results	69
Conclusions	71
References	73
 VI. SUMMARY	74
 APPENDICIES	76
Appendix A: American Chemical Society's policy on Theses and Dissertations	64
Appendix B: Author Permission Letters	66

LIST OF TABLES

Table		Page
3-1	Data Statistics for P ⁺² Structure	33
3-2	Data Statistics for P ^N Structure	34
3-3	Data Statistics for P ⁺¹ Structure	35
4-1	Product Formation of MoFe Protein Variants Using Eu(II)-L as a Reductant	50
4-S1	Data Statistics for β-98 ^{Tyr→His} MoFe Protein Structure	63
5-1	Extinction coefficients of Isolated FeMo-co in NMF.....	68

LIST OF FIGURES

Figure	Page
1-1 The Global Nitrogen Cycle	2
1-2 Molybdenum Nitrogenase	4
1-3 Binding modes of the Nitrogenase Complex	5
1-4 Metal Clusters of Molybdenum Nitrogenase	6
2-1 Effect of Osmolyte Concentration on ATP Hydrolysis and Phosphate Release	18
2-2 Log of the Rate of Reaction as a Function of Molality (m)	20
3-1 Schematic Diagram of the the Apparatus Used to Electrochemically Poise Nitrogenase Crystals	27
3-2 Visualization of the Known Structures of the P Cluster	29
3-3 The P ⁺¹ Structure	31
4-1 Nitrogenase and Metal Clusters	39
4-2 Fe Protein-Independent Hydrazine Reduction Catalyzed by MoFe Protein.....	47
4-3 Concentration Dependence of Hydrazine on MoFe Protein Substrate Reduction	48
4-4 Crystal structure of the β -98 ^{Tyr→His} variant MoFe protein.	51
4-5 Mechanical coupling among residues α -64 ^{Tyr} , β -98 ^{Tyr} , and β -99 ^{Phe} of one of the two $\alpha\beta$ units and the rest of the MoFe protein–Fe protein complex.....	53
4-6 Collective motion corresponding to the rocking of the Fe protein on the MoFe protein surface	54
4-S1 Beta factors for the nitrogenase complex.....	60
4-S2 Concentration dependence of Eu (II)-DTPA on MoFe protein substrate reduction..	61
4-S3 Covariance analysis.	62

5-1	Reduction of Carbon Dioxide to Methane and the Effect of Solvent on Activity	69
5-2	Reduction of Nitrogen Containing Substrates	70

LIST OF EQUATIONS

Equation	Page
4-1 Minimum Stoichiometry of the Nitrogenase Catalyzed Reaction	3
1-2 Redox States of the P cluster	7
2-1 Simplified Kinetic Model of the Fe Cycle of Nitrogenase	17
2-2 Correlating the Effect of Osmolyte to Conformational Change	20
4-1 Minimum Stoichiometry of the Nitrogenase Catalyzed Reaction	38
4-2 Spring Constant Function	43
4-3 Potential Energy Function.....	43
4-4 Off-Diagonal Elements of the Contact Matrix	43
4-5 Diagonal Elements of the Contact Matrix	43
4-6 Eigenvector Decomposition of the Inverse Contact Matrix	44

ABBREVIATIONS

7-meG	7-methylguanine
^{32}P -ATP	Radioactively labeled ATP on the α phosphate
[4Fe:4S]	The iron sulfur cluster of the Fe protein
[4Fe:4S] ⁺¹	The reduced state of iron sulfur cluster of the Fe protein
[4Fe:4S] ⁺²	The oxidized state of the iron sulfur cluster of the Fe protein
ADP	Adenosine diphosphate
AMPPCP	$\beta\gamma$ -methylene Adenosine Triphosphate
ATP	Adenosine Triphosphate
Apo-MoFe protein	FeMo-cofactor deficient MoFe protein
CE	Counter electrode
DTPA	Diethylenetriaminepentaacetic acid
EDTA	Ethylenediaminetetraacetic acid
EGTA	Ethyleneglycoltetraacetic acid
E _m	Midpoint potential
EPR	Electron paramagnetic resonance
ET	Electron transfer
Fe cycle	One electron transfer event from Fe to MoFe
FeFe	FeFe Nitrogenase Protein
Fe Protein	Iron protein of nitrogenase
FeMo-co	Iron molybdenum cofactor

FeMo-cofactor	Iron-molybdenum cofactor
HEPES	4-[2-hydroxyethyl]-1-piperazineethanesulfonic acid
K_m	Michaelis constant
k_{Pi}	Rate of phosphate release
k_{ET}	Rate of electron transfer
k_{ATP}	Rate of ATP hydrolysis
M cluster	Iron-molybdenum cofactor (FeMo-cofactor)
M^N	Dithionite reduced resting state of FeMo-cofactor
MOPS	3-(N-morpholino) propanesulfonic acid
MoFe protein	Molybdenum iron protein
M^{OX}	FeMo-cofactor oxidized by 1 electron from the M^N state
M^R	reduced state of FeMo-cofactor
NHE	Normal hydrogen electrode
P cluster	[8Fe-8S] cluster of MoFe protein
PBP	Phosphate binding protein
P^{1+}	P cluster in the one electron oxidized state
P^{2+}	P cluster in the two electron oxidized state
P^{3+}	P cluster in the three electron oxidized state
Pi	Inorganic phosphate
P^N	P cluster in the dithionite reduced state

PNPase	Purine nucleoside phosphorylase
P^{ox}	P cluster oxidized above the P^N state
RF	Reference Electron
SCE	Saturated calomel electrode
SDS-PAGE	Sodium dodecyl sulfate polyacrylamide gel electrophoresis
SF	Stopped-flow
UV-Vis	Ultra violet-visible
VeFe	Vanadium Nitrogenase Protein
WE	Working Electron

CHAPTER 1

INTRODUCTION

Abstract

Nitrogen (N) is used by every living organism, but only a select few have evolved to use the most abundant form of nitrogen, N_2 . This is because dinitrogen (N_2) is a very inert molecule with a very high energy barrier for reduction to ammonia (NH_3). Diazotrophs are a type of organism that are able to utilize dinitrogen as a source of nitrogen for growth, and are the major contributor of fixed nitrogen in the biological nitrogen cycle. The enzyme nitrogenase is the tool used to reduce the dinitrogen to ammonia, and the most widely studied of all nitrogenases is molybdenum dependent nitrogenase. Reduction of N_2 requires the two component proteins that make up nitrogenase to work in concert, the Fe protein and the MoFe protein. The nitrogenase enzyme has been studied extensively and the current state of knowledge on how these two proteins interact will be reviewed. Particular attention will be paid to the interaction of the Fe protein and the MoFe protein and how they function to transfer electrons into the active site of the enzyme, the iron molybdenum cofactor, as well as a review of the metal clusters that facilitate this chemistry.

Significance

As a vital component of proteins, nucleic acids, and many biomolecules, nitrogen is essential for life and is key to the survival of any organism. The largest pool of accessible nitrogen is located in the earth's atmosphere, which is composed of nearly 80% nitrogen, yet it is the limiting nutrient in many ecosystems. This is because atmospheric nitrogen is found

in the form of dinitrogen (N_2), which is not directly available for use by most living organisms.¹ Before N_2 can be utilized by most organisms it must first be “fixed” into a more reactive form of nitrogen such as protein, ammonia, or nitrate. The stability of the N_2 molecule limits its bioavailability to a group of prokaryotic microorganisms known as diazotrophs, which are able to reduce N_2 and yield two molecules of ammonia. Once nitrogen has been fixed it can be used freely by many organisms and is joined into the nitrogen cycle. The nitrogen cycle encompasses all uses of nitrogen in the biosphere in which nitrogen is oxidized, reduced, and eventually converted back to N_2 (**Figure 1-1**).

Much of the N_2 fixation that occurs annually is performed biologically via diazotrophs, a term that includes all organisms able to reduce nitrogen; while the remainder is accomplished industrially via the Haber-Bosch process.² Biological nitrogen fixation utilizes an enzymatic catalyst called nitrogenase. This catalyst contains several specialized iron sulfur clusters to input and store energy in the form of electrons, at the cost of 2 ATP per electron. There are three types of nitrogenase that differ in the composition of the active site metal. They are molybdenum nitrogenase (MoFe), vanadium nitrogenase (VFe) and iron

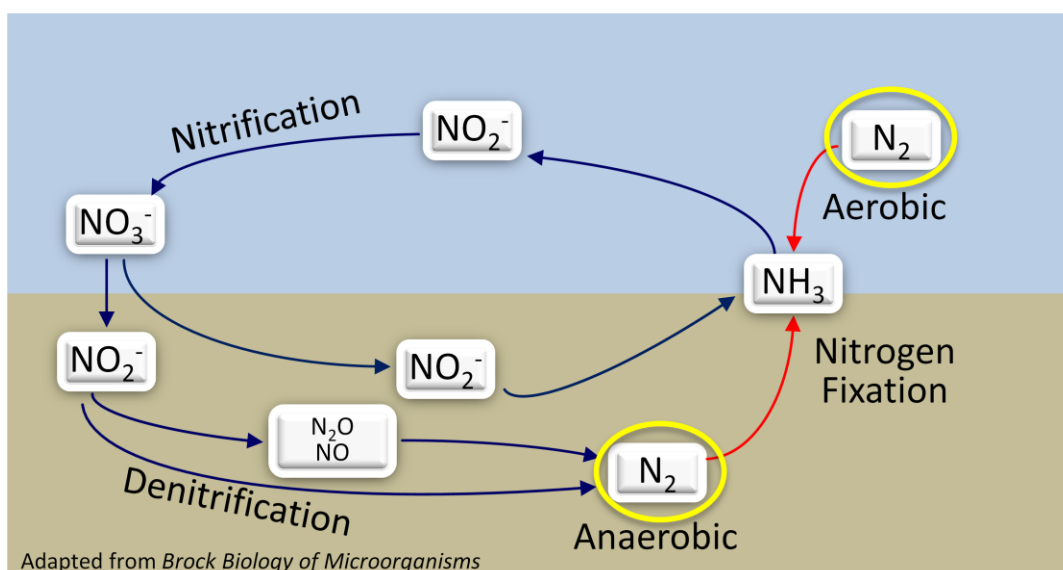
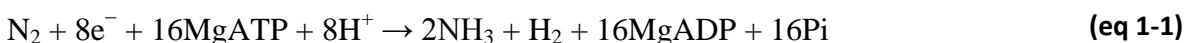


Figure 1-1 Global Nitrogen Cycle

only nitrogenase (FeFe).³ The most widely studied of these is the molybdenum nitrogenase, which is named after its active site metal cluster called the iron molybdenum cofactor (FeMo-co). FeMo-co is composed of [7Fe-9S-C-Mo-homocitrate].⁴

The reaction catalyzed by molybdenum nitrogenase can be represented in its ideal form by the equation (eq 1):



The Fe protein, also known as nitrogenase reductase, is responsible for delivering electrons to the catalytic MoFe protein, or nitrogenase (Fig 1-2). The structure of the nitrogenase complex has been determined by X-ray crystallography, revealing that the MoFe protein is an $\alpha_2\beta_2$ heterotetramer that has two catalytic subunits while the Fe protein is a homodimer.¹ During catalysis the Fe proteins dock on either end of the MoFe protein bringing the [4Fe:4S] cluster of the Fe protein in close proximity to P cluster and FeMo-cofactor of the MoFe protein. The mechanism of nitrogen reduction involves many steps, with multiple cycles of electron transfer taking place for a single N_2 being reduced. The complexity of nitrogenase presents many challenges to fully understanding the mechanism by which it reduce

Interactions of the MoFe and Fe Proteins: The Fe Cycle

Electrons are donated to the MoFe protein one at a time by the Fe protein at a cost of two ATP per electron transferred.⁵ The Fe protein contains a binding site for an ATP molecule in each subunit with a [4Fe:4S] cluster bridging the two subunits.^{1,6} The Fe protein is the biological reductant for transferring electrons to the wild type MoFe protein in a way that will support substrate reduction and participates in the reduction of nitrogen in a cyclical manner, called the Fe cycle.¹ To initiate the Fe cycle, the Fe protein needs to be in its

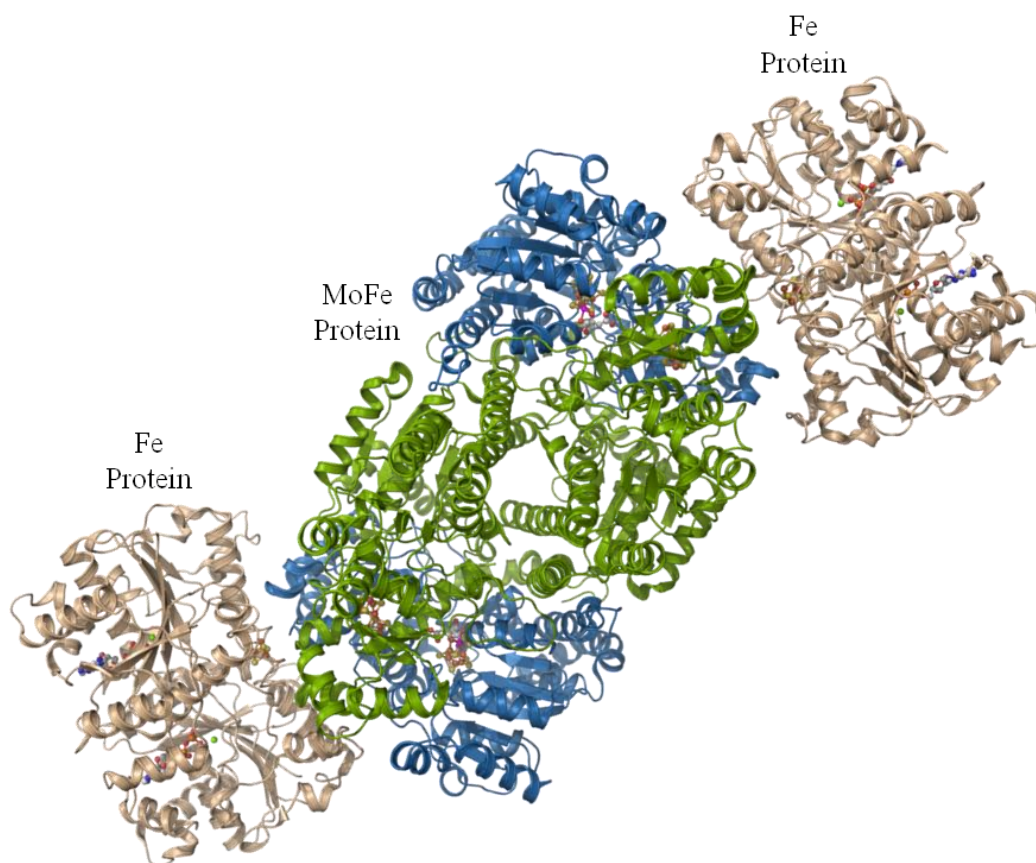


Figure 1-2. Molybdenum nitrogenase. The nitrogenase structure with ADP the bound Fe protein docked to the MoFe protein, showing both catalytic halves of the enzyme. (PDB ID 2AFI).

reduced state, with its metal cluster in the $[4\text{Fe}:4\text{S}]^{+1}$ state, and have bound two molecules of MgATP .¹ The Fe protein will then complex with the MoFe protein, transferring one electron from its metal cluster, changing the metal cluster to the $[4\text{Fe}:4\text{S}]^{+2}$ redox state, and hydrolyze two ATP before dissociating. The P cluster of MoFe protein transfers an electron to the FeMo-cofactor upon the binding of Fe to MoFe. This is followed by ATP hydrolysis, release of inorganic phosphate (Pi), and dissociation of the Fe protein.⁷

Crystallographic evidence supports the Fe protein MoFe protein complex undergoing significant structural changes during the Fe cycle. (**Figure 1-3**) The available structures demonstrate the large scale orientation changes of the Fe protein relative to the MoFe protein, though no novel internal structural variations are demonstrated. Three distinct

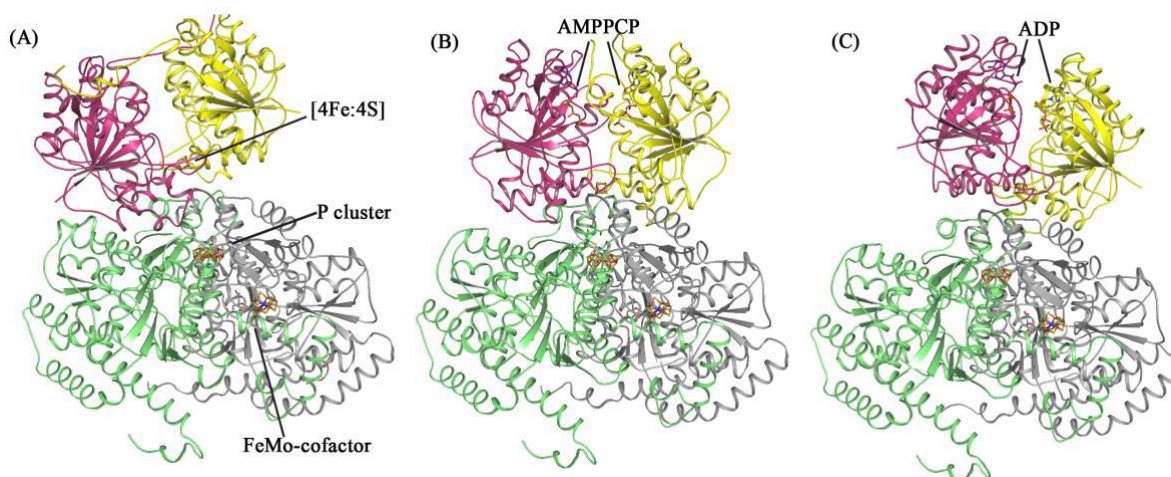


Figure 1-3. Binding modes of the nitrogenase complex. Structures depicting the Fe protein in complex with the MoFe protein with different nucleotide bound conditions: (A) nucleotide free (PDB ID 2AFH), (B) $\beta\gamma$ -methylene ATP, a non hydrolysable ATP analogue bound (PDB ID 2AFK), and (C) ADP bound form (PDB ID 2AFI). (F. A. Tezcan, J. T. Kaiser, D. Mustafi, M. Y. Waltem, J. B. Howard, D. C. Rees, *Science*. 2005, 309, 1377-1380.).

binding modes are observed, one for each of three nucleotide bound states of the Fe protein. The first is a structure achieved in the absence of nucleotides, the second is bound with a non-hydrolysable ATP analogue $\beta\gamma$ -methylene ATP, and the third state is with ADP bound to the Fe protein. This would suggest that as ATP is hydrolyzed, conformational changes occur that propagate the catalytic reaction of nitrogenase.⁸ It has been confirmed that upon Fe protein binding a conformational change must occur before electron transfer can take place. The term “conformational gating” refers to reactions that are induced by a preceding conformational change. The presence of this conformational gate validates the relevance of these distinct binding modes of the Fe protein.⁹

The Metal Clusters of Nitrogenase

The transfer of electron from the Fe protein into the active site of the MoFe protein is one of the most important steps in nitrogen reduction. There are three complex iron sulfur clusters involved in the electron transfer into the active site of nitrogenase (Figure 1-4). The simplest of these metal clusters is the [4Fe:4S] cluster of the Fe protein. The [4Fe:4S] transfers an electron to the second metal cluster, the P cluster of the MoFe protein, an

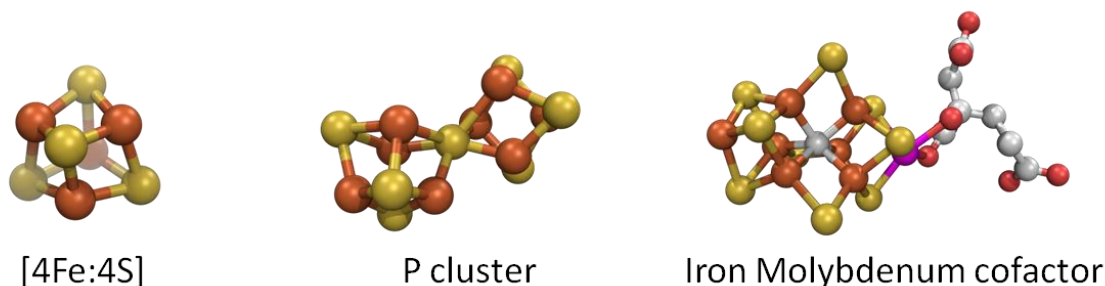
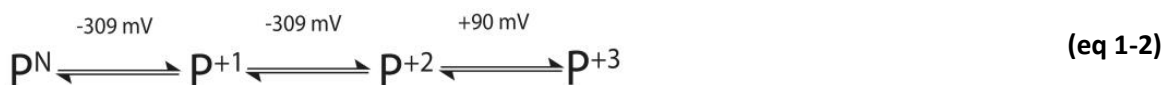


Figure 1-4. Metal Clusters of Molybdenum nitrogenase. The three metal clusters in the nitrogenase enzyme. (Left) The [4Fe:4S] cluster of the Fe protein. (Center) The [8Fe:7S] P cluster of the MoFe protein. (Right) The [7Fe-9S-C-Mo-homocitrate] FeMo-cofactor of the MoFe protein.

[8Fe:7S] cluster that acts as an intermediary in the transfer of electrons to the final cluster, the active site of nitrogenase, the iron molybdenum cofactor. The Iron molybdenum cofactor (FeMo-cofactor) is a complex iron sulfur cluster composed of [7Fe:9S:Mo:C:(R)-homocitrate].¹

Each $\alpha\beta$ subunit of nitrogenase contains both an [8Fe:7S] P cluster, which is believed to mediate electron transfer from the Fe protein to the MoFe protein, and a FeMo-cofactor. Spatially the P clusters is located between the [4Fe:4S] cluster of the Fe protein and the FeMo-cofactor of the MoFe protein, as these two metal clusters are roughly 30 Å apart. The location of the P cluster is perfectly situated to facilitate and electron transfer event between the two.¹ The P cluster is known to exhibit four distinct electronic states that can be achieved by the addition of various redox mediators to achieve the requisite potential of that redox state (eq 1-2).¹



Understanding the redox chemistry of the P cluster is vital to understanding its role in nitrogen reduction, and many studies have been performed in order to better understand which redox states the P cluster accesses during catalysis. As the P^{+3} cannot be returned to the P^{+2} in vitro, it is assumed that this state is not a biologically important state. Thus researchers have focused on whether the $P^{+1/N}$ or the $P^{+2/+1}$ redox couple are biologically relevant. These two redox couples can transfer either one or two electrons to the FeMo-

cofactor from the P cluster. Both the $P^{N/+1}$ and the $P^{+1/+2}$ couples exhibit redox potentials which are similar to each other at -300mV suggesting that either could perform the requisite electron transfer.^{1, 10} The oxidized states of the P cluster, P^{+1} and P^{+2} , can be observed using EPR spectroscopy, while the P^N resting state is EPR silent. Unfortunately, while P^{+1} and P^{+2} are paramagnetic, and thus have an observable EPR spectrum, they are difficult to observe during turnover, preventing a detailed knowledge of the state of the P cluster during catalysis.¹

The working model for the P cluster function during catalysis is that the P cluster starts in the all ferrous state P^N , which is the resting state observed *in vitro* under dithionite reducing condition. Upon Fe protein binding one electron is known to be transferred to the FeMo-cofactor leaving the P^{+1} state, thus the $P^{N/+1}$ electronic couple is thought to be the biologically relevant state of the P cluster during catalysis.¹

One model for the P cluster's role in nitrogenase is called deficit spending. Deficit spending states that the association of the Fe protein to the MoFe protein triggers an electron transfer event that is conformationally gated in which the P cluster transfers an electron to the FeMo-cofactor.² The P cluster would now be in the one electron oxidized P^{+1} with a deficit of one electron, having started at the P^N resting state and transferred one electron.. This deficit would then be rapidly filled by an intermolecular electron transfer event from the reduced [4Fe-4S] cluster in the Fe protein to the P cluster, restoring the P cluster to the P^N state.¹¹ This model explains why the oxidized forms of P cluster are never observed, as the reduction of the oxidized P cluster by the Fe protein would be much faster than the conformationally gated transfer of electron to the MoFe protein, thus preventing an accumulation of P^{OX} .¹¹

Much of the work in this thesis pertains to the P cluster and understanding what changes it undergoes during catalysis. This is important in understanding how the nitrogenase regulates electron flow into the active site FeMo-cofactor to build up sufficient energy to reduce the N₂ triple bond.

The FeMo-cofactor [7Fe-9S-Mo-C-Homocitrate] of nitrogenase is a complex metal cluster composed of two cubanes held together with an interstitial carbide and three bridging sulfides. One of these cubanes contains the molybdenum atom attached to the homocitrate tail, which is coordinated to the protein through its 2-hydroxy and 2-carbonyl groups. FeMo-cofactor is attached to the protein by a Fe atom bound to $\alpha 275^{\text{Cys}}$ and the Mo atom bound to $\alpha 442^{\text{His}}$ of the MoFe protein. Evidence shows that the FeMo-cofactor is the active site of nitrogenase where substrate binding and reduction takes place.¹

Understanding how FeMo-co accumulates electrons and reduces substrate is one of the central questions for understanding the mechanism of nitrogenase, and could lead to development of synthetic catalysts to mimic this behavior. In order to better understand the cofactor, it has been extracted into organic solvents, isolating it from the protein and the other metal clusters.¹² The isolated cofactor was then studied spectroscopically under many conditions to determine its behavior. These studies have been limited in their utility as the cofactor displayed very limited catalytic ability in its isolated form.

The isolated cofactor was first shown to interact with a glassy carbon electrode connected to a potentiostat to produce hydrogen gas, but electrochemical reduction of more complex substrates proved difficult to achieve.¹³ More successfully, a chemical reductant Eu(II)-DTPA with a midpoint potential of -1.14V, has been shown to support cyanide

reduction to ammonia and methane, as well as carbon monoxide reduction to methane.

These results, while exciting, are still very limited, as the turnover number is very low, often below one.¹⁴ Using more potent reductants, such as a Sm(II)I₂ with a midpoint potential of -1.8V, gives better results, as well as expanding the range of substrates to include carbon dioxide.¹⁵

Now that a reaction has been discovered in which FeMo-co reduces substrate, studies can determine which conditions favor catalytic turnover of FeMo-cofactor, leading to a better understanding of how this complex metal cluster works. This could potentially guide the design of novel synthetic catalysts. The final section of this thesis is devoted to understanding which conditions favor FeMo-co activity, and how to modulate that activity to favor certain substrates over others as targets for reduction.

Electron Transfer in Nitrogenase

The P- cluster and FeMo-cofactor have been discussed, but electron transfer is controlled in large part by the Fe protein. As discussed earlier the Fe protein is a homodimer with a bridging [4Fe:4S] cluster. This cluster is both structural, maintaining the integrity of the homodimer, as well as functional, as the metal cluster has 3 available oxidation states, allowing it to transfer electrons. The Fe protein is the intermediary between metabolic electrons, such as flavodoxins and ferodoxins *in vivo*, and sodium dithionite *in vitro*, and the nitrogenase MoFe protein. The Fe protein is the only reductant that can support activity with the unaltered wild type MoFe nitrogenase, and the only reductant that can support nitrogen reduction.¹ Though a nitrogenase variant has been constructed that will allow substrate

reduction using a small molecule chemical reductant, it does not support the reduction of nitrogen.¹⁶

The midpoint potential of the $\text{Fe}^{+1}/\text{Fe}^{+2}$ couple is dependent on the nucleotide bound state of the Fe protein. Fe protein can exist in three different nucleotide bound states, no nucleotide bound, ATP bound, and ADP bound, with the midpoint potentials from -300mV in the absence of nucleotide, to -420 mV when bound to ATP, and -440 mV when bound to ADP. Though both the ATP and ADP bound forms of Fe protein can achieve a very low redox potential, only the ATP bound iron protein will transfer electrons to the MoFe protein.¹⁷

The structure of the ATP bound Fe protein varies significantly from the no nucleotide bound state. Upon binding ATP the [4Fe:4S] cluster of the Fe protein undergoes a 5 Å shift towards the surface of the protein. This shift puts the cluster in much closer proximity to the P cluster upon binding the MoFe protein, facilitating electron transfer.¹⁷

Summary

Research into nitrogenase is ongoing and exciting, and there are many important questions left to answer. By understanding how nature performs complex and difficult chemical reactions in such an efficient manner, new techniques may be developed that mimic these reactions on an industrial scale. In order to find these answers the key question of nitrogenase must first be answered. How are electrons transferred into and through the nitrogenase enzyme? What role do conformational changes play in electron transfer and substrate reduction? How does nitrogenase regulate the flow of electrons into the active site metal cluster? How does the FeMo-cofactor of nitrogenase utilize this energy to reduce

substrate? Is there any way to regulate the activity of the isolated Iron Molybdenum cofactor in order to tune its reactivity towards other substrates? These questions are dealt with in part by this thesis, and much work remains to be done in order to fully understand nitrogenase.

REFERENCES

- (1) Seefeldt L. C., Hoffman B. M., Dean D. R., (2009) *Annu. Rev. Biochem.*, 78, 701-722.
- (2) Smil V., (2001) *Cambridge, MA: MIT Press*. Enriching the Earth: Fritz Haber, Carl Bosch, and the Transformation of World Food Production.
- (3) Eady R. R., (1996) *Chem Review*. 96, 3013-3030.
- (4) Lancaster K. M., Roemelt M., Ethenhuber P., Hu Y., Ribbe M. W., Neese F., Bergmann U., DeBeer S., (2011) *Science.*, 334, 974-977.
- (5) Howard J. B., D. Rees C., (1996) *Chem. Review*. 96, 2965-2982.
- (6) Georgiadis M. M., Koniya H., Chakrabarti P., Woo D., Kornuc J. J., Rees D. C., (1992) *Science.*, 257, 1653-1659.
- (7) Duval S., Danyal K., Shaw S., Lytle A. K., Dean D., Hoffman B. M., Antony E., Seefeldt L. C. (2013) *PNAS*. 16414-16419.
- (8) Tezcan F. A., Kaiser J. T., Mustaf D. i, Waltem M. Y., Howard J. B., Rees D. C. (2005) *Science*. 309, 1377-1380.
- (9) Danyal K., Mayweather D., Dean D., Hoffman B. M., Seefeldt L. C. (2010) *JACS*. 20, 6894-6895.
- (10) Lanzilotta W. N., Christiansen J., Dean D. R., Seefeldt L. C. (1998) *Biochemistry*. 212, 51-61.
- (11) Danyal K., Dean D., Hoffman B. M., Seefeldt L. C. (2011) *Biochemistry*. 43, 9255-9263.
- (12) McClean P. A., Wink D. A., Shapmen S. K., Hickman A. B., McKillop D. M., Orme-Johnson W. H. (1989) *Biochemistry*. 28, 9402-406.

- (13) Gall T., Ibrahim S., Gormal C., Smith B., Pickett C. J. (1999) *Chem. Comm.* 9, 773-774.
- (14) Lee C., Hu Y., Ribbe M. W. (2012) *Angewandte Chemie*.51, 1947-1949.
- (15) Rebelein J., Hu Y., Ribbe M. W. (2014) *Angewandte Chemie*. 53, 11543-11546.
- (16) Danyal K., Dean D., Hoffman B. M., Seefeldt L. C. (2011) *Biochemistry*.50, 9255-9263.
- (17) Jang S. B., Seefeldt L. C., Peters J. W. (2000) *Biochemistry*.39, 1-8.

CHAPTER 2

CONFORMATIONAL GATING OF THE ATP HYDROLYSIS AND PHOSPHATE
RELEASE STEPS OF THE Fe CYCLE**Abstract**

The Fe protein of nitrogenase contains a [4Fe-4S] cluster and delivers electrons one at a time to the MoFe protein during turnover. The Fe protein is in the [4Fe-4S]¹⁺ reduced state (Fe^{red}) and bound to two MgATP when it complexes with the MoFe protein. The transfer of one electron to the MoFe protein from the Fe protein is coupled to the hydrolysis of two molecules of ATP. Crystal structures of the nitrogenase complex show a large variability in the way in which the Fe protein docks on the surface of the MoFe protein, the different docking modes are dependent upon whether the Fe protein is bound to a nucleotide, and to which nucleotide (ATP or ADP) Fe protein has bound. This finding suggest that intermolecular electron transfer (ET) from the Fe protein to MoFe protein is “gated”, or regulated, by conformational changes of the complex or of its component proteins.¹ This has been proven true in a study looking closely at the primary electron transfer event. This study demonstrated an inhibition of rate of electron transfer as a function of increasing molality (m) of the solution. This inhibition was used to extrapolate the extent to which this step of electron transfer was dependent upon a conformational change taking place in the protein. It was concluded that a conformational change on the order of 800 Å² takes place before electron transfer may occur.

The different binding modes of the Fe protein suggest that there could be more than one important conformational change occurring.¹ The remaining event in the Fe cycle, ATP

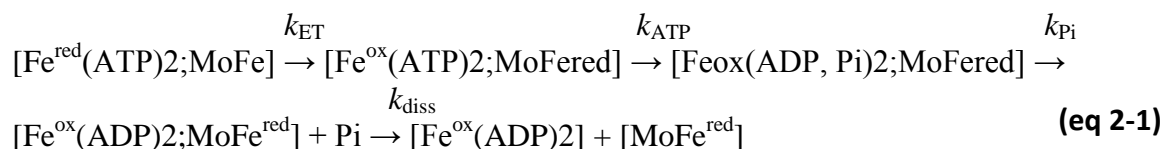
hydrolysis, release of inorganic phosphate, and dissociation of the Fe protein have not been investigated. Here we discuss the evidence that there are indeed at least two additional conformational gates in the Fe cycle of nitrogenase, regulating both ATP hydrolysis, and phosphate release.

Experimental Procedures

Materials, Protein Purification and Activity Assays: All reagents, unless stated otherwise, were purchased from Sigma Aldrich Chemicals (St. Louis, MO). Nitrogenase proteins were expressed in *Azotobacter vinelandii* strain DJ995 (WT MoFe with 7X His tag), and DJ884 (WT Fe protein) as previously described.² MoFe protein was purified using ion metal affinity chromatography as previously described.² Fe protein was purified using ion exchange and size-exclusion liquid chromatography.² Both proteins were greater than 95% pure based on sodium dodecyl sulfate-polyacrylamide gel electrophoresis separation followed by Coomassie blue staining. Proteins were kept in septum-sealed serum vials under argon atmosphere. All gases and liquids were transfers using gastight syringes.

Quench Flow Studies for ATP Hydrolysis: Pre-steady ATP hydrolysis assays were performed at 25°C on a rapid chemical quench-flow instrument (KinTek Corp, Austin, TX) housed in a glove box under a nitrogen atmosphere. A 18 µL volume of 10 µM MoFe and 20 µM Fe (syringe A) was mixed with a 18 µL volume of 1 mM ATP with [α -¹⁴² ³²P]ATP (1.5 µCi) from syringe B, with varying times of reaction. Reactions were rapidly quenched with 45 µL of 0.5 M EDTA added from syringe C. All buffers contained the given osmolytes, sucrose or glycerol, at the appropriate molality (m). Aliquots (0.9 µL) of the quenched reaction were spotted onto a thin layer chromatography (TLC) plate and developed in 0.6 M

potassium phosphate buffer, pH 3.4 for 75 minutes. The [α - ^{32}P]ATP and the [α - ^{32}P]ADP were detected with a Storm PhosphorImager (Molecular dynamics, Sunnyvale, CA) and quantified using the ImageQuant software (Molecular Dynamics, Sunnyvale, CA). The data were fit to the model (eq 2-1), with the values of the non ATP hydrolysis variable fixed to



accepted values of $k_{\text{ET}} = 140 \text{ s}^{-1}$, $k_{\text{Pi}} = 16 \text{ s}^{-1}$, $k_{\text{diss}} = 6 \text{ s}^{-1}$.³

Where, k_{ET} , k_{ATP} , k_{Pi} and k_{diss} are the rates constants for ET, ATP hydrolysis, phosphate release, and $[\text{Fe}^{\text{ox}}(\text{ADP})_2;\text{MoFe}]$ complex dissociation, respectively.³

Kinetics of Inorganic Phosphate Release: The time-course of phosphate release was performed using a stopped-flow (Auto SF-120, Kintek Corp, Austin, TX) using the coumarin (N-[2-(1-maleimidyl)ethyl]-7-(diethylamino) coumarin-3-carboxamide) labeled phosphate binding protein assay (MDCC-PBP).⁴ This is accomplished when Pi binding to MDCC-PBP results in an increase in fluorescence ($\lambda_{\text{excitation}} = 430 \text{ nm}$, $\lambda_{\text{emission}} > 450 \text{ nm}$).⁴ These experiments were performed at 25°C in buffer containing 0.5 mM sodium dithionite and 25 mM HEPES at pH 7.4 and the indicated amount of osmolyte, sucrose or PEG 300. It is imperative that the molalities of both solutions to be mixed are as close as possible, as schlieren effects can cause artifacts that distort the early time points. Prior to the experiments all buffers, syringes, and the stopped flow lines were treated with a Pi-MOP (SF-buffer with 300 μM 7-methylguanine (7-meG), and 0.2 units/ml purine nucleoside phosphorylase (PNPase) for 15 min to remove contaminating Pi.⁴ A solution of 2 μM MoFe and 6 μM Fe

was mixed with a solution of 10 μM PBP-MDCC, 20 mM MgCl_2 and 2mM ATP in the stopped flow and the change in fluorescence was monitored over time. These experiments were repeated with multiple concentrations of the osmolytes. PBPMDCC fluorescence enhancement was converted to $[\text{Pi}]$ after calibration in the stopped flow using $[\text{NaH}_2\text{PO}_4]$ standards as described.⁴ The Pi release data were fit to the sequential kinetic model (eq 2-1) with $k_{\text{ET}} = 140 \text{ s}^{-1}$, $k_{\text{ATP}} = 70 \text{ s}^{-1}$, and $k_{\text{diss}} = 6 \text{ s}^{-1}$ fixed.³

Results and Discussions

To determine whether conformational gating plays a role in the ATP hydrolysis and phosphate release event, osmolytes were added to the reaction at different molalities in order to determine the effect on rate. The osmolytes used were sucrose and PEG 300 for phosphate release, with sucrose glycerol and being used for ATP hydrolysis with molalities ranging up

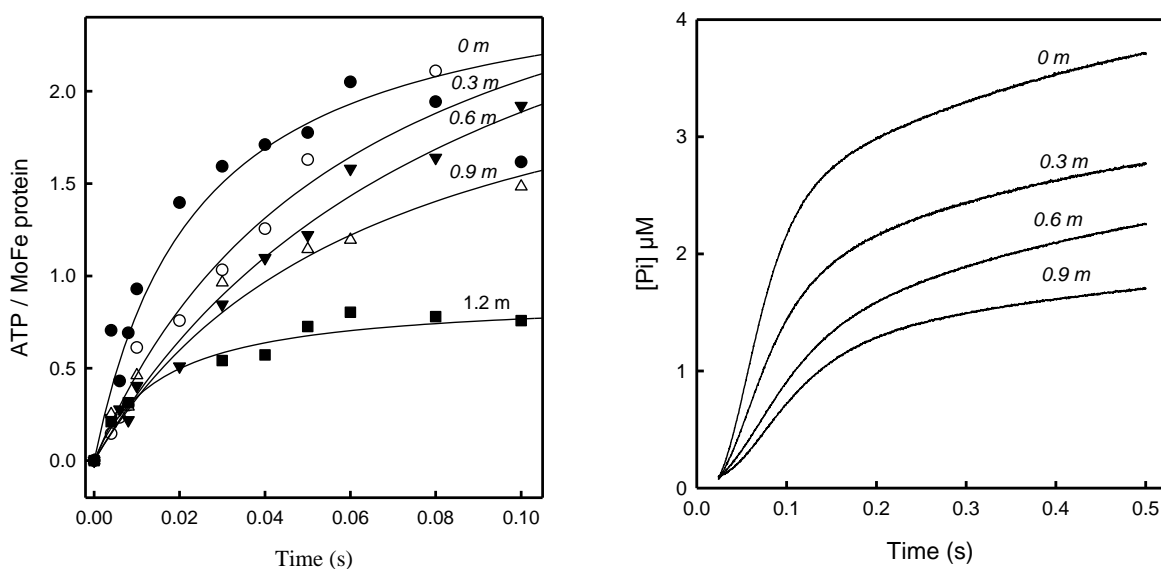


Figure 2-1. Effect of Osmolyte Concentration on ATP Hydrolysis and Phosphate Release. (left) ATP hydrolyzed / MoFe Protein over time as a function of increasing sucrose concentration. (Right) as with left but monitoring phosphate release.

to 1.2 m. The sucrose data is shown for both ATP hydrolysis and Pi release (Fig 2-1)

Plotting the log rates of reaction as a function of osmolyte concentration yields a line, the slope of which corresponds to the number of waters involved in the conformational change of the reaction.⁵ (Fig 2-3) Taking this data we can see that there is decidedly an effect due to the addition of the osmolytes, and that it corresponds to a conformational change.⁵

When k_{ATP} or k_{Pi} are controlled by osmotic pressure, the slope of k vs. m is proportional to $[-\Delta n]$, which corresponds to the number of waters involved in the conformational change according to eq 2-1.⁶ As the slopes are negative we can infer an uptake of water molecules. Multiple osmolytes were employed to calculate the slope because different osmolytes will interact with the protein surface in different ways, yielding different values for Δn .⁶ The osmolyte with the steepest slope is the most accurate value to use, as it interferes least with the protein.⁷ Sucrose was the best osmolyte in both of these studies, and the slopes for ATP hydrolysis and phosphate release respectively yielded a $\Delta n \approx 120$ and 160 as a reasonable estimate to the number of waters that the protein uptakes during these conformational transitions.

Conclusions

There are two possible explanations for the effect seen when adding an osmolyte to solution. As the concentration of osmolyte increases so too does the viscosity of the reaction buffer, which could slow the rate of reaction down. The other possibility is that the osmolyte itself could be the cause of the rate decrease by interacting directly with the protein, by displacing waters interacting with the surface of the protein. An effect due to the osmolyte will only be observed when the protein must undergo a conformation change before the event

in question takes place, causing the protein to displace or uptake water molecules, which have now been replaced by the osmolyte in question. It has been shown that the effect seen here is nearly entirely due to the presence of the osmolyte hindering a conformational

$$k(m) \propto e^{[-(\Delta n/55.6)m]} \quad (\text{eq 2-2})$$

change, rather than due to viscosity.⁵ The effect molality has on rate is described in eq. 2-2.

Where $k(m)$, Δn , and m are the rate of reaction at a given molality, the number of waters involved in the conformational change, and the molality of the osmolytes in solution.⁵

Here is shown that further conformational changes beyond what was previously

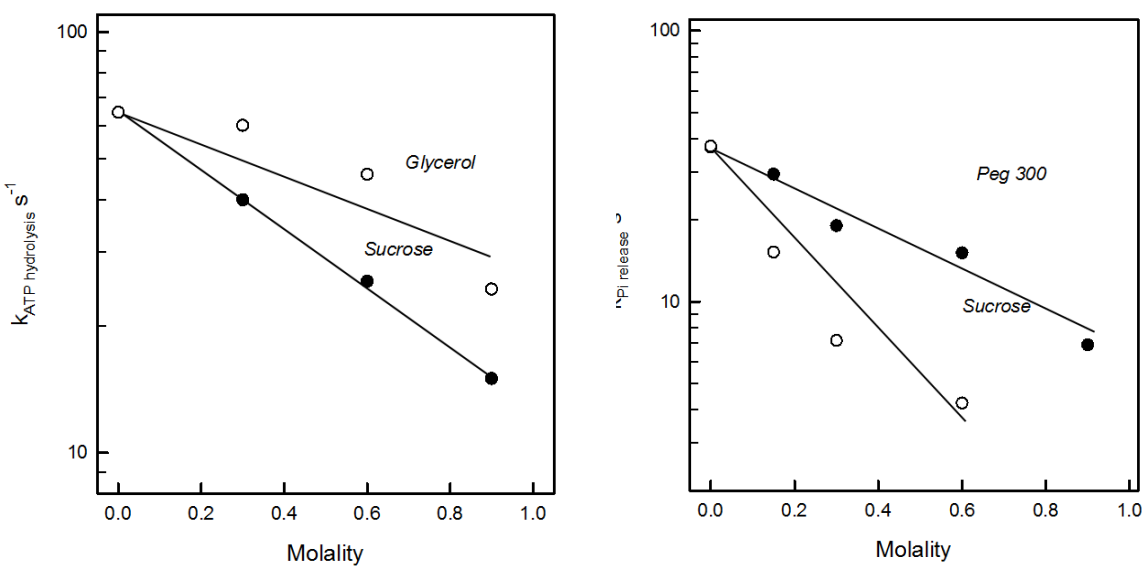


Figure 2-2. Log of the Rate of Reaction as a Function of Molality (m). (left) Log plot of the rate of ATP hydrolysis during pre-steady state catalysis of the nitrogenase complex as a function of sucrose and Glycerol concentration (m). (right) Log plot of the rate of phosphate release as a function of sucrose and PEG 300 concentration (m).

reported to take place before ATP hydrolysis occurs, and even further changes take place before allowing the release of inorganic phosphate. Thus both the ATP hydrolysis event and the phosphate release event are gated by conformational changes in the protein as the Fe cycle progresses.

The magnitude of the conformational changes observed in this study taken together is equal to what was previously shown. Each of the waters involved in a conformational change correlates to roughly 10 \AA^2 , so we see that the calculated conformational change of 120 waters is about equal to a $1,200 \text{ \AA}^2$ change in all the steps up to and including ATP hydrolysis. When we take the data from phosphate release we see that there are now nearly 160 waters involved, correlating to a conformational change of roughly $1,600 \text{ \AA}^2$ occurs.⁵ The previous study found that the magnitude of the conformational change involved in primary electron transfer encompassed roughly 800 \AA^2 , leaving the magnitude of the conformational change needing to occur after primary electron transfer but before the ATP hydrolysis event to be 400 \AA^2 , with another 400 \AA^2 conformational change needing to occur before the phosphate release event.

This evidence of the control of every detail of the Fe cycle suggests that the precise regulation of every event in electron transfer is needed in order to optimize the efficiency of the MoFe protein. It is possible that these events are so tightly controlled in order to prevent access to the FeMo-cofactor after it has been activated by the transfer of electrons from the Fe protein. Keeping FeMo-co isolated is important to prevent waste of reducing equivalents, thus wasting energy.

REFERENCES

- (1) Tezcan F. A., Kaiser J. T., Mustafi D., Waltem M. Y., Howard J. B., Rees D. C. (2005) *Science*. 09, 1377-1380.
- (2) Lanzilotta W. N., Christiansen J., Dean D. R., Seefeldt L. C. (1998) *Biochemistry* 37, 11376–11384.
- (3) Duval S., Danyal K., Shaw S., Lytle A. K., Dean D., Hoffman B. M., Antony E., Seefeldt L. C. (2013) *PNAS*. 41, 16414-16419.
- (4) Brune M., Hunter J. L., Corrie J. E., Webb M. R. (1994) *Biochemistry*. 247, 6214-6219.
- (5) Danyal K., Mayweather D., Dean D., Hoffman B. M., Seefeldt L. C. (2010) *American Chemical Society*. 135, 6894-6895
- (6) Parsegian V. A., Rand R. P., Rua D. C. (1995) *Methods Enzymol*. 259, 43-94.
- (7) Dougherty R. C. (2001) *J. Phys. Chem*. 105, 4514-4519.

CHAPTER 3

ELECTROCHEMICALLY POISING THE P CLUSTER OF NITROGENASE AT DEFINED POTENTIALS: CAPTURING THE STRUCTURE OF AN ELECTRON TRANSFER INTERMEDIATE

Abstract

The nitrogenase enzyme functions to catalyze the activation and cleavage of the di-nitrogen bond leading to the formation of ammonia. A series of ATP dependent electron transfer events facilitate this catalysis. The P cluster, an intermediary [8Fe-7S] cluster in the nitrogenase enzyme, has been shown to be involved in electron transfer. The P cluster has been reported to undergo redox dependent conformational changes as it fluctuates between P^N , P^{+1} , and the P^{+2} states. Previous structural investigations have identified two distinct P cluster conformations that correspond to spectroscopically observed P^N and P^{+2} states, however, the catalytically important P^{+1} state has yet to be visualized. A novel technique to poise nitrogenase protein crystals at defined electrochemical potentials was developed to structurally characterize the P^{+1} state of the P cluster. This result represents a major advance towards understanding the mechanism of electron transfer of the nitrogenase enzyme, and is relevant in the study of how electron flow is regulated in nitrogenase.

Nitrogenase is responsible for the multiple electron reduction of atmospheric nitrogen gas to ammonia. This complex oxygen sensitive metallo-protein system undergoes a series of ATP dependent single electron transfer events between the electron donor Fe protein, and the catalytically active MoFe protein. During catalysis, the process of electron delivery to the active site involves two types of electron transfer events: one event being the

intermolecular electron transfer between the [4Fe-4S] cluster of the Fe protein and the P cluster of the MoFe protein, and the other being the intramolecular electron transfer between the P cluster and the [7Fe-9S-C-Mo-homocitrate] FeMo-cofactor active sites within the MoFe protein.¹ Recent work has helped to determine the order of these electron transfer events with a proposed "deficit-spending" model. This model postulates that the interaction of the Fe protein and the MoFe protein elicit conformational changes that facilitate an initial "slow" step that is conformationally gated. This step is the electron transfer event between the P cluster and the FeMo-cofactor.² After transferring one electron, the P cluster is left with a "deficit" of one electron, and has been designated P^{1+} , relative to the P^N designated all-ferrous resting state. The initial electron transfer event has been measured to take place at a rate of 140 s^{-1} .² This deficit is then rapidly filled by a second "fast step," the intermolecular electron transfer event from the reduced $[4\text{Fe-4S}]^{1+}$ cluster in the Fe protein to the P cluster, restoring the P^N state.² This fast step is a direct electron transfer step and takes place at rates greater than 1700 s^{-1} which could explain why P^{ox} has never been spectroscopically observed during turnover.² Thus the deficit spending model postulates that major conformational changes occur during the Fe cycle, but the conformational changes that regulate the electron flow are short-lived. This may explain why crystal structural analyses of multiple nitrogenase protein complexes have not yielded any significant insight into this aspect of the mechanism. While the mechanistically relevant P^{1+} state has been observed spectroscopically in WT and variant MoFe proteins, this state was only achievable using electrochemical mediators.^{3,4} Structurally, this state has not previously been characterized due to its short lived nature during catalysis., nor has it been successfully observed under catalytic turnover conditions, leaving the state of the P^{+1} P cluster a mystery.

Previous investigations have reported two distinct structures of the P cluster, which correspond well to the spectroscopically assigned P^N resting state and P^{2+} oxidized state.⁵ The structural change observed by the two-electron difference revealed a rearrangement of inorganic P cluster atoms and altered covalent coordination to the surrounding protein amino acid residues. The P^{2+} conformation is typically seen in native MoFe crystals structures, while the P^N state was observed by reducing MoFe crystals with excess sodium dithionite just prior to flash cooling in a similar manner to spectroscopic studies.^{3,5} Although these two states are structurally accessible, evidence indicates that the relevant electron transfer event occurs between the reduced P^N state P cluster and the active site, suggesting the P^{1+} state is the biologically relevant state of the P cluster under turnover conditions.² The P^N and P^{2+} structures provide fascinating insight into the redox dependent structural changes that the P cluster can undergo, but provide little information into the nature of the catalytically relevant P^{1+} state, or at what potential this redox conformational change occurs. A novel technique was developed to poise nitrogenase protein crystals at defined midpoint potentials using redox mediated solutions controlled by a potentiostat to probe for redox induced changes in the P cluster.

Experimental Procedures

All chemicals were purchased from Sigma-Aldrich (St. Louis, MO) or Fischer Scientific (Fair Lawn, NJ) and were used without further purification. Wild type MoFe protein from *Azotobacter vinelandii*, DJ995, was purified under strict anaerobic conditions with slight modifications to previously described protocols.⁶ All proteins were obtained at greater than 95% purity as judged by SDS-PAGE analysis using Coomassie blue staining and

demonstrated full specific activity (greater than 2,000 nmolH₂/min/mg protein). Handling of proteins was done in septum-sealed serum vials under an argon atmosphere. All transfers of gases and liquids were done using gastight syringes. Protein crystals were grown by capillary batch diffusion in a 100% N₂ atmosphere MBraun glove box with previously reported precipitant solutions.⁷ Crystals were harvested anaerobically under an argon stream and immobilized on pins using a novel “sandwich” loop design to prevent the crystals from washing away during electrochemical studies. Two micromesh loops (MiTiGen) were affixed on top of each other to the same pin, and a small piece of monofilament was placed in between to pry them apart. Crystals were positioned between the loops, and the monofilament was then removed to apply tension from the loops to secure the crystals. The immobilized crystals were immediately submerged in an electrode solution mimicking the precipitant solution composed of 18% PEG 4000, 60mM Tris buffer pH 8.0, 15% glycerol, 100mM sodium chloride, and 1 mM of a redox mediator.

The mediators used were methylene blue (MB), indigo disulfonate (IDS) flavin mononucleotide (FMN), benzyl viologen, and methyl viologen (MV). These solutions were degassed and placed in an electrochemical cell with a built in glassy carbon working electrode (WE) (2.8 cm² surface area), a built in platinum counter electrode (CE), and a saturated calomel reference electrode (SCE). The solutions were kept under a constant stream of Argon to maintain anaerobicity.

The electrode solutions were poised at +11 mV, -120 mV, -238 mV, -360 mV and -488 mV vs. standard hydrogen electrode for MB, IDS, FMN, BV and MV respectively. An OMNI-101 microprocessor controlled potentiostat (Cypress Systems. Lawrence, Kansas) was

used to control potential and constant stirring was used to achieve a uniform solution. The submerged sandwich looped crystals were allowed to soak for 1 hour and were immediately flash cooled in liquid nitrogen to preserve the poised states (Fig 3-1).

Data was collected at SSRL BL12-2 and crystal structures of wild type MoFe protein poised at five defined potentials, with the best three, +11, -240, and -450 refining to at least 2.2 Å (Table 3-2). Due to the increased susceptibility to radiation damage caused by the mediator solution treatment, partial data sets were collected to observe unaltered structural features, and a decrease in data quality was observed relative to untreated crystals. Refined structures were compared with previously published MoFe structures to probe for evidence

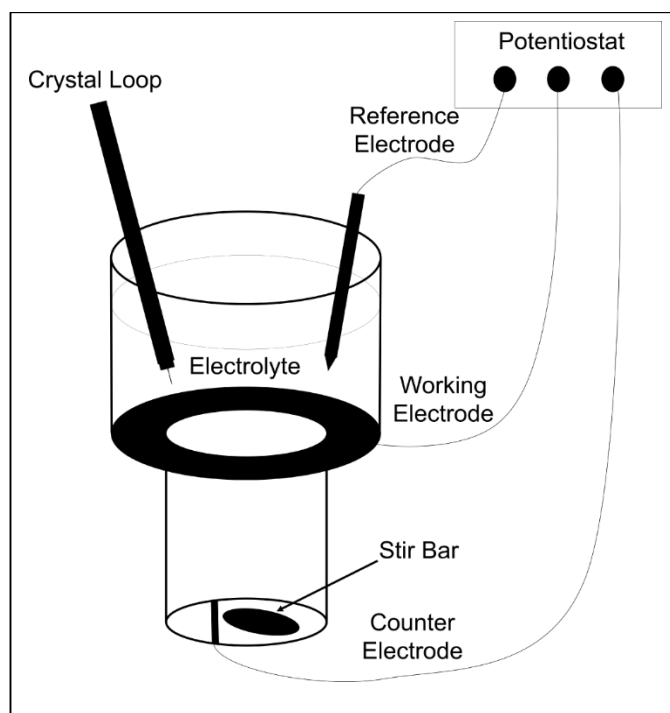


Figure 3-1. Schematic Diagram of the the Apparatus Used to Electrochemically Poise Nitrogenase Crystals. Crystals were submerged in a stirred soution held at constant potential for 1 hour prior to flash cooling in liquid nitrogen.

of redox induced structural changes to the P cluster.⁵ Crystal structures of crystals treated with MV held at -488 mV and BV at -360 mV for one hour showed the P^N state of the P cluster indicating that they were reduced by the mediator. Furthermore, crystal structures of crystals treated with MB held at +11 mV and IDS held at -120 for one hour showed the oxidized P^{OX} state of the P cluster observed in untreated crystals. Crystallographic analysis of MoFe crystals treated with FMN held at -238 mV (a midpoint between the oxidized and reduced structures) for one hour revealed a novel intermediate structure we have designated the P⁺¹ state based on inferences from previous spectroscopic investigations (Fig 3-2).

Results and Discussions

The one electron oxidized P⁺¹ state P cluster shares structural features of both the P^N and P^{OX} nitrogenase structures (3MIN and 2MIN respectively).⁵ The P⁺¹ state structure can be described as a mixture of the P^N and P^{OX} states in that the cluster is coordinated by the side chain oxygen Ser-β188 to Fe6 like to the P^{OX} state, but is no longer coordinated to the backbone nitrogen of Cys-α88 to Fe5 similar to the P^N state (Fig 3). The internal structural differences also display an intermediate state between the P^N and P^{OX} clusters, in that Fe5 remains bonded to S1 similar to the P^N state and Fe6 is moved out of bonding distance from S1 similar to the P^{OX} structure. All of the iron atoms in the P cluster both in the P^N and P⁺¹ state remain four-coordinate, with the major difference being the exchange of a serinate ligand for an internal sulfur-iron bond between Fe6 and S1.

This P^{+1} state structure reinforces the proposed deficit spending mechanism and demonstrates a redox-mediated ligand exchange mechanism for possibly regulating electron flow between the $P^N - P^{1+}$ redox couple. The idea of using a conformational change to transiently force a ligand on to a metal cluster in order to lower its midpoint potential has been proposed before and is called a “compound gate” mechanism.⁹ Previous mutagenesis

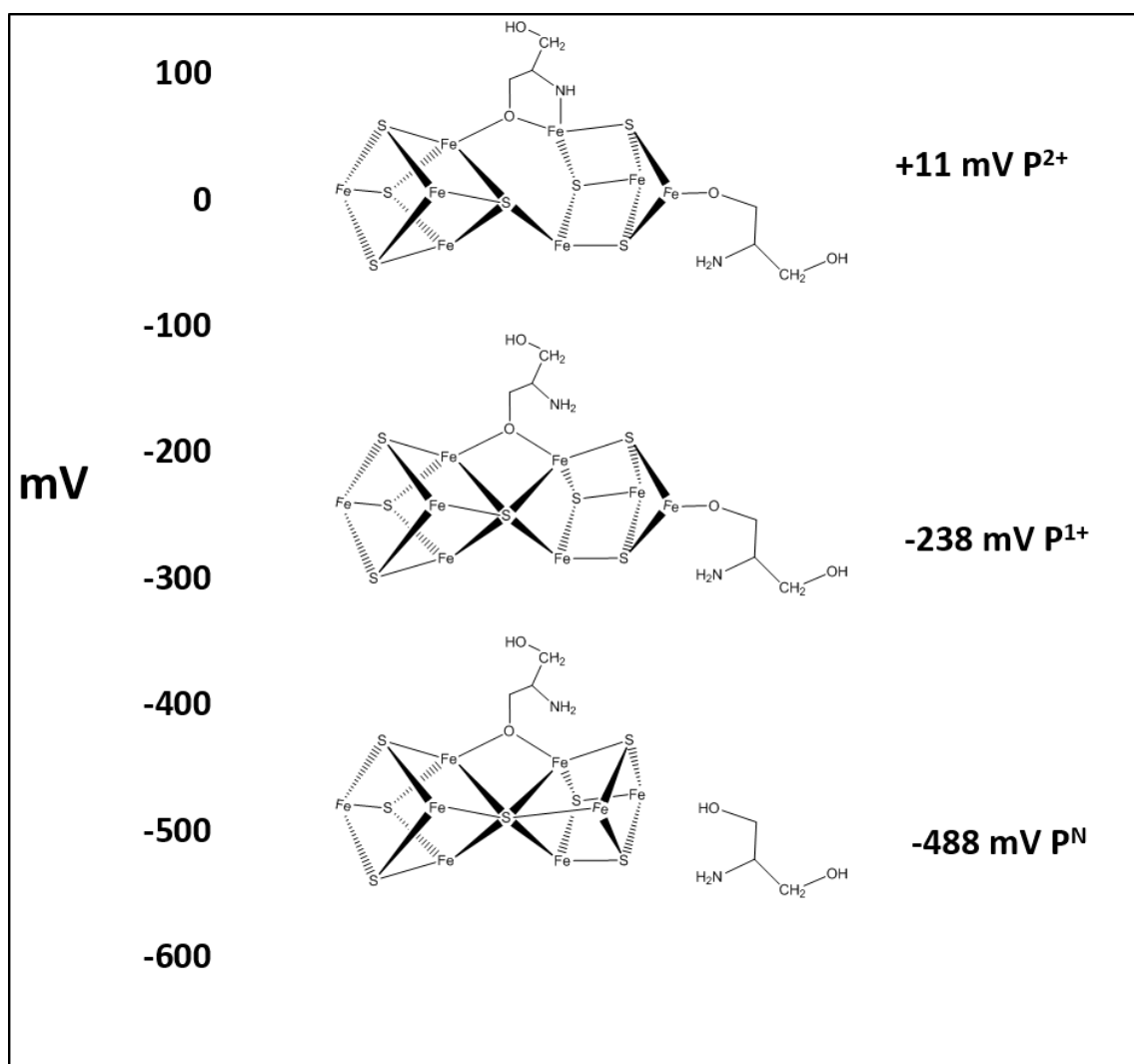


Figure 3-2. Visualization of the Known Structures of the P Cluster. Representation of the three distinct states of the P cluster that were captured at different potentials. The P^{+1} intermediate is a novel structure.

studies targeting the Ser- β 188 P cluster ligand imply introduction of a stronger ligand, such as cysteine, or removal of coordination by glycine substitution stabilize the P cluster in the P^{+1} and P^N states by shifting the resting potential of the cluster -90 mV and +60 mV respectively.⁴ Also of interest is these mutations confer lower specific activities to the variants by disrupting a key exchangeable ligand.^{2,4} These observations add support to our P^{+1} assignment of this structure and the prominence of a ligand exchange mechanism in nitrogenase catalysis. We have recently shown that electron transfer between the Fe protein and the MoFe protein precedes ATP hydrolysis.¹¹ Conformational changes within the P cluster of the MoFe protein during the deficit spending events could potentially serve as triggers for the initiation of the ATP hydrolysis step within the Fe protein. This would result in the Fe protein cycle of electron transfer being a tightly and mechanically/conformationally controlled series of events.

The one electron ligand exchange also raises the possibility of the P cluster's involvement in the proposed proton coupled electron transfer mechanism in nitrogenase. The Ser- β 188 ligand will be protonated when not coordinated to the P cluster, and sequential hydride formation has been postulated as part of the catalytic cycle, therefore the single redox P^N - P^{+1} couple fits intuitively well into the most recent proposed mechanism.¹³ Additionally, previous spectroscopic studies have also shown residues around the distal P cluster cubane to be involved in proton coupled electron transfer.¹² Although this unique iron-sulfur cluster has been shown to undergo unprecedented redox-mediated structural changes, a complete understanding of the unidirectional proton coupled electron transfer is difficult without more information regarding the complex and dynamic global conformational changes that occur when the Fe protein interacts with the MoFe protein.

Current structural techniques have failed to provide us with the details of these transient global conformational changes. By utilizing a new redox crystallography approach, we are now able to take a snapshot of one of these short-lived states and piece together the details of one of nature's most enigmatic catalytic cycles. The work presented here also has relevance to probing redox states of not only nitrogenase but numerous metalloprotein systems, and may lead to exciting advances in our understanding of biological electron transfer.

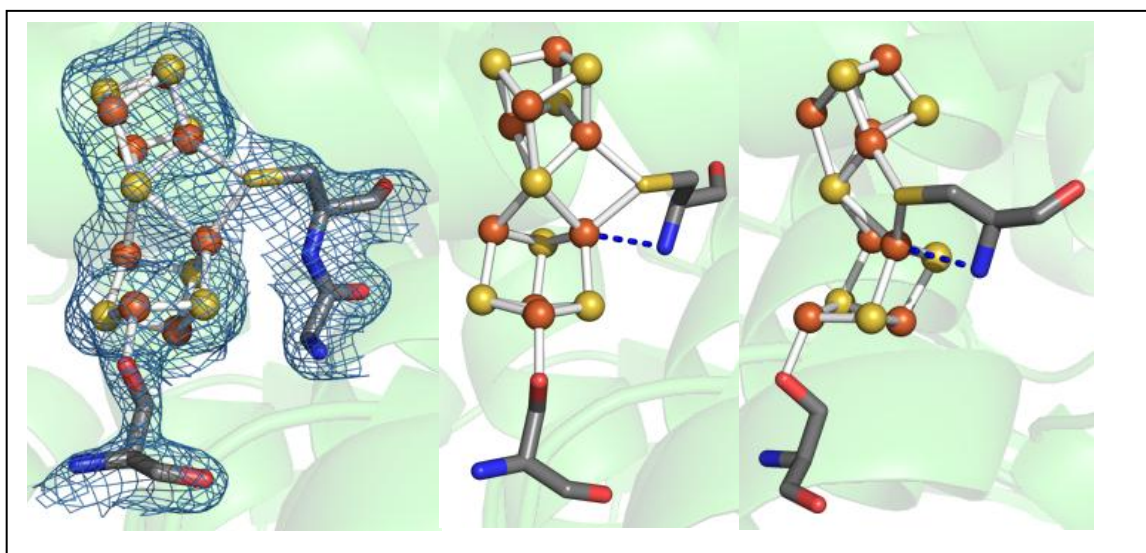


Figure 3-3. The P^{+1} Structure. (Left) $2F_o-F_c$ electron density contoured to 2.0 sigma highlighting an absence of coordination by the amide nitrogen of α -88^{Cys}. (Middle, Right) 90° of the P cluster with transient global conformational changes. Fe6 distance is 1.9Å.

Acknowledgments

The work presented in this chapter was a collaborative effort between people with many specialties and is not all my work. Stephen Keable, working in John Peters' group at Montana State University, did everything to do with crystallography, from growing the crystals and designing the sandwich loops to refining the X-ray crystal structures.

Karamatullah Danyal was there at the beginning of this project, and was instrumental in developing the techniques used to soak and poise the crystals at the target potentials. My role in this work was to design, set up, and maintain the electrochemical cell at the correct potential to poise the crystals at the correct potentials during the soaking of the crystals. Without their help this work would never have been completed.

Table 3-1: Data Statistics for P+2 Structure

cell dimensions	a = 81.18 Å b = 130.99 Å c = 107.85 Å $\alpha = \gamma = 90.00^\circ$ b = 110.77
space group	P21
wavelength	$\lambda_1 = 0.97947$
resolution(Å)	50-2.10
completeness (%)	67.7 (68.9) ^b
obsd reflections	197146
unique reflections	95737
Avg redundancy	2.1
I/ σ	4.6 (1.5) ^b
Rsym(%)	13.2 (42.8) ^b
CC(1/2)	0.994 (0.816)
Refinement Statistics	
Resolution (Å)	50-2.0
R _c (R _{cryst}) (%)	20.42
R _{free} (%)	23.74
Real Space CC _d (%)	
Mean B Value (overall; Å ²)	18.5
Coordinate Error (based on maximum likelihood, Å)	0.19
RMSD from ideality:	
Bonds (Å)	0.036
Angles (°)	4.361
Ramchandran Plot:	
Most favored (%)	94.9
Additional allowed (%)	4.49
Outliers (%)	0.61

^b Numbers in parenthesis refer to the highest resolution shell.

$c_{ry} = 100 * \sum |I_i(h) - \langle I(h) \rangle| / \sum I_i(h)$ where $I_i(h)$ is the i th measurement of reflection h and $\langle I(h) \rangle$ is the average value of the reflection intensity
 $c_{Rcryst} = \sum |F_o| - |F_c| / \sum |F_o|$ where F_o and F_c are the observed and calculated structure factor amplitudes used in refinement. R_{free} is calculated as R_{cryst} , but using the "test" set of structure factor amplitudes that were withheld from refinement. d Correlation coefficient (CC) is agreement between the model and $2mF_o - DF_c$ electron density map. e Calculated using Molprobit (25)

Table 3-2: Data Statistics for PN Structure

cell dimensions	a = 79.09 Å b = 132.81 Å c = 108.77 Å $\alpha = \gamma = 90.00^\circ$ b = 109.45
space group	P21
wavelength	$\lambda_1 = 0.97947$
resolution(Å)	50-2.2
completeness (%)	53.1 (57.5)b
obsd reflections	107763
unique reflections	56701
Avg redundancy	1.9
I/ σ	5.9 (2.0) b
Rsym(%)	8.8 (38.8) b
CC(1/2)	.992(.340)
Refinement Statistics	
Resolution (Å)	50-2.2
R _{cryst} (%)	25.44
R _{free} (%)	29.62
Real Space CC _d (%)	92.5
Mean B Value (overall; Å ²)	17.99
Coordinate Error (based on maximum likelihood, Å)	0.37
RMSD from ideality:	
Bonds (Å)	0.019
Angles (°)	4.144
Ramchandran Plot:	
Most favored (%)	92.11
Additional allowed (%)	6.59
Outliers (%)	1.31

b Numbers in parenthesis refer to the highest resolution shell.

$cR_{sym} = 100 * \sum |I_i(h) - \langle I(h) \rangle| / \sum I_i(h)$ where $I_i(h)$ is the i th measurement of reflection h and $\langle I(h) \rangle$ is the average value of the reflection intensity. $cR_{cryst} = \sum ||F_o| - |F_c|| / \sum |F_o|$ where F_o and F_c are the observed and calculated structure factor amplitudes used in refinement. R_{free} is calculated as R_{cryst} , but using the "test" set of structure factor amplitudes that were withheld from refinement. d Correlation coefficient (CC) is agreement between the model and $2mF_o - DF_c$ electron density map. e Calculated using Molprobit (25)

Table 3-3: Data Statistics for P+1 Structure

cell dimensions	a = 80.79 Å b = 130.78 Å c = 107.88 Å $\alpha = \gamma = 90.00^\circ$ b = 110.85
space group	P21
wavelength	$\lambda_1 = 0.97947$
resolution(Å)	50-2.10
completeness (%)	57.06 (60.8)b
obsd reflections	150869
unique reflections	70560
Avg redundancy	2.1
I/ σ	4.0 (1.3) b
Rsym(%)	14.2 (54.4) b
CC(1/2)	0.992 (0.814)
Refinement Statistics	
Resolution (Å)	50-2.0
R _c cryst (%)	23.46
R _{free} (%)	26.58
Real Space CC _d (%)	
Mean B Value (overall; Å ²)	40.49
Coordinate Error (based on maximum likelihood, Å)	0.21
RMSD from ideality:	
Bonds (Å)	0.017
Angles (°)	3.993
Ramchandran Plot:	
Most favored (%)	94.92
Additional allowed (%)	4.67
Outliers (%)	0.4

b Numbers in parenthesis refer to the highest resolution shell.

$cR_{sym} = 100 * \sum |I_i(h) - \langle I(h) \rangle| / \sum I_i(h)$ where $I_i(h)$ is the i th measurement of reflection h and $\langle I(h) \rangle$ is the average value of the reflection intensity. $cR_{cryst} = \sum ||F_o| - |F_c|| / \sum |F_o|$ where F_o and F_c are the observed and calculated structure factor amplitudes used in refinement. R_{free} is calculated as R_{cryst} , but using the "test" set of structure factor amplitudes that were withheld from refinement.

dCorrelation coefficient (CC) is agreement between the model and $2mF_o - DF_c$ electron density map. eCalculated using Molprobit (25)

REFERENCES

- (1) Seefeldt L. C., Hoffman B. M., Dean D. R., (2009) *Annu. Rev. Biochem.* 78, 701–722.
- (2) Danyal K., Dean D. R., Hoffman B. M., Seefeldt L. C. (2011) *Biochemistry* 50, 9255–9263.
- (3) Tittsworth R. C., Hales B. J. (1993) *J. Am. Chem. Soc.* 115, 9763–9767.
- (4) Chan J. M., Christiansen J., Dean D. R., Seefeldt L. C. (1999) *Biochemistry* 38, 5779–5785.
- (5) Peters J. W., Stowell M. H. B., Soltis S. M., Finnegan M. G., Johnson M. K., Rees D. C. (1997) *Biochemistry* 36, 1181–1187.
- (6) Christiansen J., Goodwin P. J., Lanzilotta W. N., Seefeldt L. C., Dean D. R. (1998) *Biochemistry* 37, 12611–12623.
- (7) Sarma R., Barney B. M., Keable S., Dean D. R., Seefeldt L. C., Peters J. W. (2010) *J. Inorg. Biochem.* 104, 385–389.
- (8) Danyal K., Inglet B. S., Vincent K. A., Barney B. M., Hoffman B. M., Armstrong F. A., Dean D. R., Seefeldt L. C. (2010) *J. Am. Chem. Soc.* 132, 13197–13199.
- (9) Peters J. W., Stowell M. H., Soltis S. M., Finnegan M. G., Johnson M. K., Rees D. C. (1997) *Biochemistry* 36, 1181–1187.
- (10) Yang Z. Y., Danyal K., Seefeldt L. C. (2011) *Methods Mol. Biol. Clifton NJ* 766, 9–29.
- (11) Duval S., Danyal K., Shaw S., Lytle A. K., Dean D. R., Hoffman B. M., Antony E., Seefeldt L. C. (2013) *Proc. Natl. Acad. Sci.* 110, 16414–16419.
- (12) Lanzilotta W. N., Christiansen J., Dean D. R., Seefeldt L. C. (1998) *Biochemistry* 37, 11376–11384.

CHAPTER 4

Fe PROTEIN-INDEPENDANT SUBSTRATE REDUCTION BY NITROGENASE MoFe

PROTEIN VARIANTS

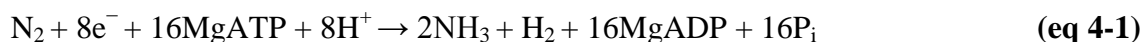
Abstract

The reduction of substrates catalyzed by nitrogenase normally requires nucleotide-dependent Fe protein delivery of electrons to the MoFe protein, which contains the active site FeMo cofactor. Here, it is reported that independent substitution of three amino acids (β -98^{Tyr→His}, α -64^{Tyr→His}, and β -99^{Phe→His}) located between the P cluster and FeMo cofactor within the MoFe protein endows it with the ability to reduce protons to H₂, azide to ammonia, and hydrazine to ammonia without the need for Fe protein or ATP. Instead, electrons can be provided by the low-potential reductant polyaminocarboxylate-ligated Eu(II) (E_m values of -1.1 to -0.84 V vs. the normal hydrogen electrode). The crystal structure of the β -98^{Tyr→His} variant MoFe protein was determined, revealing only small changes near the amino acid substitution that affect the solvent structure and the immediate vicinity between the P cluster and the FeMo cofactor, with no global conformational changes observed. Computational normal-mode analysis of the nitrogenase complex reveals coupling in the motions of the Fe protein and the region of the MoFe protein with these three amino acids, which suggests a possible mechanism for how Fe protein might communicate subtle changes deep within the MoFe protein that profoundly affect intramolecular electron transfer and

*Coauthored by Karamatullah Danyal, Andrew J. Rasmussen, Stephen M. Keable, Sudipta Shaw, Oleg A. Zadornyy, Simon Duval, Dennis R. Dean, Simone Raugei, John W. Peters, and Lance C. Seefeldt (2015) *Biochemistry* 54 (15), pp 2456-2462. Copyright 2015 American Chemical Society. Reprinted with Permission.

substrate reduction

Mo-dependent nitrogenase catalyzes the fixation of biological dinitrogen (N_2) to ammonia (NH_3) with the minimum reaction stoichiometry shown in eq 1:^{1,2}



Nitrogenase consists of two component proteins called the iron (Fe) protein and the molybdenum–iron (MoFe) protein (Figure 1).¹ The MoFe protein is an $\alpha_2\beta_2$ heterotetramer consisting of two catalytic $\alpha\beta$ units, each containing a P cluster [8Fe-7S] and a FeMo cofactor (FeMo-co; [7Fe-9S-1Mo-Chomocitrate]).^{3,4} The Fe protein is a homodimer with a [4Fe4S] cluster bridging the two subunits and an ATP binding site on each subunit.⁵ To achieve the complete reduction of N_2 at FeMo-co in the MoFe protein, a Fe protein must transiently bind to the MoFe protein.⁶ During this association of the two proteins, a single electron is passed from the Fe protein to FeMo-co, followed by the hydrolysis of the two ATP molecules bound to the Fe protein.⁷ Recent evidence suggests that the electron transfer reaction proceeds in two steps with the first step being transfer of an electron from the P cluster to FeMo-co, followed by transfer of an electron from the Fe protein to the oxidized P cluster (termed a “deficit spending” electron transfer mechanism).⁸ ATP hydrolysis follows the electron transfer events, with release of the P_i and finally dissociation of the Fe protein from the MoFe protein.^{7,9} The two ADP molecules bound to the released Fe protein are exchanged with ATP, and the oxidized Fe protein is reduced by dithionite (in vitro) or flavodoxin/ferredoxin (in vivo).^{1,10} This catalytic cycle is repeated eight times to achieve the accumulation of sufficient electrons for the activation and reduction of N_2 and the stoichiometric release of H_2 .^{1,2}

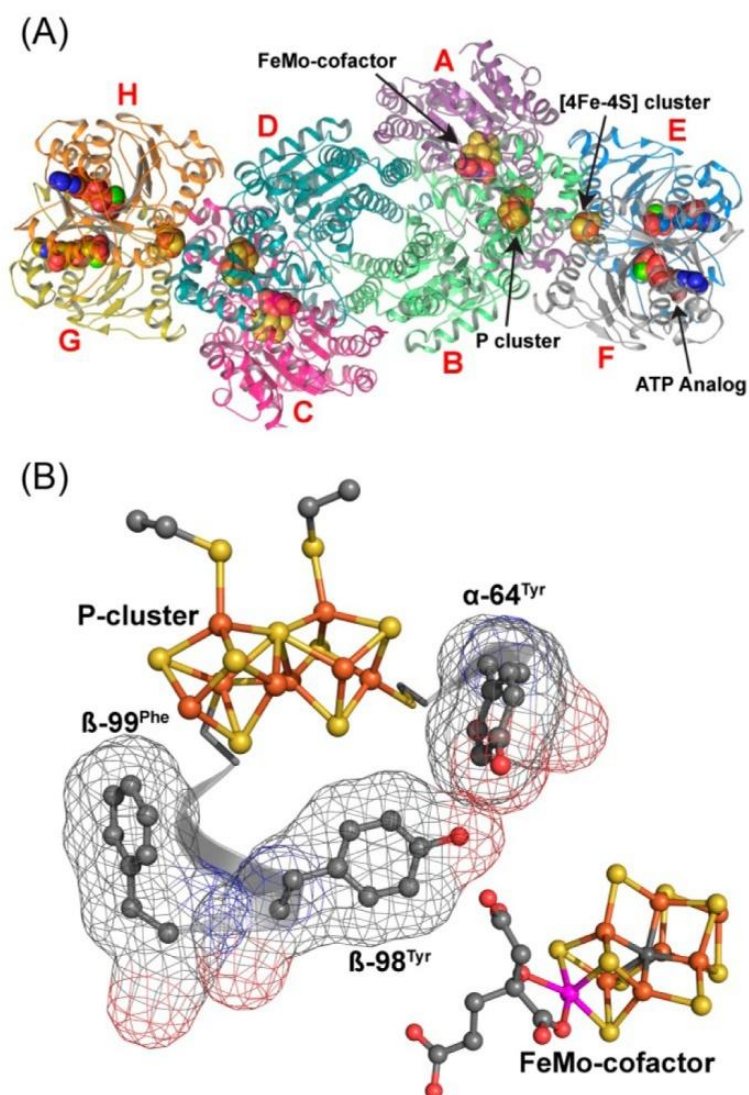


Figure 4-1. Nitrogenase and Metal Clusters. (A) Structure of the nitrogenase complex (PDB entry 2AFK). Each unit is labeled from A to H according to the PDB numbering. (B) Three amino acid residues relevant to the Fe protein-independent reduction of the substrates (N_2H_4 , N_3^- , and H^+) by the MoFe protein shown in ball and stick representation with the mesh representing the van der Waals surface. Also shown are the P cluster and FeMo-co in ball and stick representation. The linkage from $\alpha-64^{Tyr}$ to the P cluster ligand $\alpha 62^{Cys}$ and from $\beta-98^{Tyr}$ to the P cluster ligand $\beta-95^{Cys}$ are also shown. Atom colors are rust for Fe, yellow for S, gray for C, red for O, and magenta for Mo.

Fe protein is the only reductant known to support N_2 reduction by the MoFe protein, suggesting it plays a pivotal role in the mechanism beyond simply donating electrons. Two recent reports have revealed that it is possible to deliver electrons directly to the MoFe protein in the absence of the Fe protein with reduction of a few substrates other than N_2 . In one case, a Ru–ligand complex was covalently attached to the MoFe protein, and it was possible to photo induce transfer of an electron into the MoFe protein to achieve very low rates of reduction of the nonphysiological substrate acetylene to ethylene and cyanide to methane.^{11,12} In another case, substitution of a single amino acid within the MoFe protein located between the P cluster and FeMo-co (β -98^{Tyr→His}) allowed a Eu–ligand complex in solution to deliver electrons to the MoFe protein to achieve reduction of hydrazine to ammonia at rates near those observed when electrons are delivered from the Fe protein.¹³ This finding suggested that amino acids located between the P cluster and FeMo cofactor within the MoFe protein might play an important but poorly understood role in regulating electron transfer events that support substrate reduction at FeMo-co.

Here, we report that independent substitution of three amino acids co-located between the P cluster and FeMo-co (β 98Tyr→His, α -64Tyr→His, and β -99Phe→His) endows the resultant MoFe proteins with the ability to reduce the substrates hydrazine, azide, and H^+ at significant rates using Eu(II) ligands as a reductant without the need for the Fe protein. The crystal structure of the β -98^{Tyr→His} MoFe protein was determined, revealing subtle conformational changes and altered solvent structure in the proximity of FeMo-co. These small changes between the P cluster and FeMo-co may mimic conformational changes requisite for catalysis. Calculations conducted on the Fe protein–MoFe protein complex reveal a mechanical coupling between the Fe protein and the region containing the β -98^{Tyr}, α -

64^{Tyr} , and β -99^{Phe} amino acids within the MoFe protein, providing a possible mechanism for the communication between the Fe protein and key determinants of MoFe protein intramolecular electron transfer.

Experimental Procedures

Materials, Protein Purification, and Activity Assays. All reagents, unless stated otherwise, were purchased from SigmaAldrich Chemicals (St. Louis, MO). MoFe proteins were expressed in *Azotobacter vinelandii* strains DJ939 (β -98^{Tyr→His}), DJ1956 (β -99^{Phe→His}), and DJ1957 (α -64^{Tyr→His}) that were grown as described previously.¹⁴ The MoFe proteins from each strain were purified, with some modifications, as described to >95% purity and confirmed by sodium dodecyl sulfate– polyacrylamide gel electrophoresis analysis using Coomassie blue staining.¹⁴ Manipulation of proteins was done in septum sealed serum vials under an argon atmosphere. All transfers of gases and liquids were conducted using gastight syringes. Azide reduction, H₂ evolution, and N₂H₄ reduction activities were determined as described previously.¹⁵ NH₃ was quantified using a fluorescence method with o-phthalaldehyde as described previously.¹⁵ For all assays, Eu(II)-L was generated by electrochemical reduction, as described previously.¹⁶

Crystallization. Crystallization trials were performed on β 98^{Tyr→His} MoFe protein that was concentrated to ~30 mg/ml and stored in the purification buffer. All trials were conducted under anaerobic conditions in a nitrogen atmosphere glove box (UniLAB, M. Braun) using a micro capillary batch diffusion method.^{17,18} Crystallization was accomplished as previously described using a precipitating solution that contained 30% polyethylene glycol (PEG) 4000, 100 mM Tris-HCl (pH 8.0), 190 mM sodium molybdate, and 1 mM sodium

dithionite.¹⁹ Crystals of a dark brown color with the approximate dimensions of $100\ \mu\text{m} \times 200\ \mu\text{m} \times 200\ \mu\text{m}$ were observed after they had grown for 4–6 weeks. The crystals were cryoprotected by diffusion of mother liquor doped with ~15% glycerol. Crystals were harvested under a stream of continuous argon on rayon loops and immediately flash-cooled in liquid nitrogen. Data were collected on beamline BL-9-2 at the Stanford Synchrotron Radiation Laboratory under a continuous flow of liquid nitrogen at ~100 K. A data set was collected at $\lambda = 0.97$ on a MAR 325 detector up to resolution $1.97\ \text{\AA}$ and was scaled and integrated using the HKL2000 software package.²⁰

The unit cell parameters of the collected data were nearly isomorphous to the published native structure (PDB entry 3U7Q). Initial rigid body fitting and refinement were performed using AutoMR of the CCP4 suite of programs.²¹ Calculation of electron density maps and model fitting were accomplished by using Coot, and the model was refined using REFMAC5 to $1.97\ \text{\AA}$ resolution.²² The final model was built with a crystallographic R of 21.5, with 95.6% of the residues in the most favored Ramachandran regions and 4.2% in additionally allowed regions (Table S1 of the Supporting Information). The PDBeFold Structure Similarity server at the European Bioinformatics Institute (<http://www.ebi.ac.uk/msdsrv/ssm/>) was used to determine an average root-mean-square deviation (rmsd) of $0.2\ \text{\AA}$ between analogous α -carbons of the β -98^{Tyr→His} MoFe variant and the wild-type MoFe structure (PDB entry 3U7Q).

Normal-Mode Analysis. To characterize the mechanical aspects of the long time scale dynamics of the nitrogenase complex, we performed a normal-mode analysis based on the anisotropic Gaussian network model.^{23,24} The nitrogenase complex was represented by beads centered at the position of the α -carbons. According to this model, two beads are connected

with a harmonic spring if they are within a cutoff distance, R_{cut} , and not connected otherwise.

To improve the stability of the model, in this study the force constant, k , of the spring was chosen to vary smoothly from k_0 to zero using the sigmoidal switching function around R_{cut}

$$k(r_{ij}) = \frac{k_0}{1 + e^{(r_{ij} - R_{\text{cut}})/\gamma}} \quad (\text{eq 4-2})$$

given in eq 4-2.^{25,26}

where r_{ij} is the distance between beads i and j and γ is the width of the switching function.

We used a cutoff distance R_{cut} of 12 Å, with a width for the switching function of 2 Å.

Different choices gave consistent results, in agreement with previous reports.²⁵

According to this model, the potential energy function of the protein is given by eq 4-3:

$$V = \frac{1}{2} \sum_{i,j=1}^N \sum_{\alpha,\beta=x,y,z} k(r_{ij}) \Delta r_i^\alpha \Gamma_{ij}^{\alpha\beta} \Delta r_j^\beta \quad (\text{eq 4-3})$$

where Δr_i^α is the α component ($\alpha = x, y, \text{ and } z$) of position vector \mathbf{r}_i for the i th α -carbon and Γ is the so-called contact matrix. The off-diagonal and diagonal elements of the contact matrix are given by eq 4-4 and 4-5, respectively:

$$\Gamma_{ij}^{\alpha\beta} = \frac{k(r_{ij})}{k_0} \frac{\mathbf{r}_i \cdot \mathbf{e}_\alpha}{|\mathbf{r}_i|} \frac{\mathbf{r}_j \cdot \mathbf{e}_\beta}{|\mathbf{r}_j|} \quad (\text{eq 4-4})$$

$$L_{\alpha\alpha}^{\parallel} = - \sum_{\substack{\beta=1 \\ \beta \neq \alpha}}^{\beta=N} \sum_{\substack{\gamma=1 \\ \gamma \neq \alpha}}^{\gamma=N} L_{\alpha\beta}^{\parallel} - \sum_{\substack{\beta=1 \\ \beta \neq \alpha}}^{\beta=N} L_{\alpha\beta}^{\parallel} \quad (\text{eq 4-5})$$

where \mathbf{e}_α is the unit vector along Cartesian direction α . The correlations between the fluctuations of the protein residues were analyzed in terms of the covariance matrix C , whose elements $C_{ij} = \sum_\alpha \langle \Delta r_i^\alpha \Delta r_j^\alpha \rangle$ were calculated from the eigenvector decomposition of the inverse of the contact matrix (eq 4-6):²⁴

$$C_{ij} = \frac{3k_B T}{k_0} \sum_\alpha [\Gamma^{-1}]_{ij}^{\alpha\alpha} = \frac{3k_B T}{k_0} \sum_{k=7}^{3N} \sum_\alpha \lambda_k^{-1} [\mathbf{v}_k \cdot \mathbf{v}_k^T]_{ij}^{\alpha\alpha} \quad (\text{eq 4-6})$$

where λ_k and \mathbf{v}_k are the k^{th} eigenvalue and eigenvector of the contact matrix, respectively. The six zero-frequency modes corresponding to rigid body translations and rotations of the nitrogenase complex are excluded from the summation over the normal modes. Diagonal elements of the covariance matrix are proportional to the β factor of the amino acid residues, $\beta_i = 8\pi^2 C_{ii}/3$. As one can see in eq 4-6, the spring constant k_0 acts as a mere scaling factor for the atomic fluctuations and the β factors, and its value was chosen to reproduce the average magnitude of the crystallographic β factors. The model is able to reproduce faithfully the relative magnitude of the experimental β factors (Figure 4-S1 of the Supporting Information), making us confident that it is also able to describe the overall large amplitude motions of the nitrogenase complex.

The calculations were performed on the crystal structure of the complex between the Fe protein and the MoFe protein from *Azotobacter vinelandii* with an ATP analogue and ADP bound to the Fe protein (PDB entries 2AFK and 2AFI, respectively).²⁷

Results and Discussions

The recent preliminary finding that substitution of β -98^{Tyr→His} in the MoFe protein allows it to reduce hydrazine to ammonia without participation of the Fe protein or ATP, but instead with electrons coming from Eu(II)-DTPA, points to participation of the protein around β -98^{Tyr} in the MoFe protein in regulating electron transfer between the P cluster and FeMo-co or in the reactivity of FeMo-co.¹³ To further explore this possibility, we have prepared MoFe proteins having independent amino acid substitutions for three amino acids co-localized between the P cluster and FeMo-co (β -98^{Tyr→His}, β -99^{Phe→His}, and α -64^{Tyr→His}) (Figure 4-1). The amino acid substitutions did lower the proton reduction to H₂ rate driven by the Fe protein and ATP to 1100 ± 25 nmol of H₂ min⁻¹ mg⁻¹ for β -98^{Tyr→His} and to below detection for the β -99^{Phe→His} and α -64^{Tyr→His} variants. The wildtype rate is ~ 2000 nmol of H₂ min⁻¹ (mg of MoFe protein)⁻¹. The three variant MoFe proteins were tested for their ability to reduce substrates without Fe protein, but instead with electrons coming from Eu(II) ligands. For these assays, Eu(II) and DTPA were added simultaneously to initiate the assay with no Fe protein added. Figure 2 shows the time dependence for the reduction of hydrazine (N₂H₄) to ammonia (NH₃) for the three variant proteins with rates ranging from 167 to 708 nmol of NH₃/mg of MoFe protein over 25 min. Activity was dependent on addition of Eu(II), DTPA, hydrazine, and MoFe protein. The reduction of hydrazine (N₂H₄) is a unique property of these variant MoFe proteins compared to the wildtype MoFe protein alone, which is unable to reduce hydrazine with Eu-L as an electron donor.

When the hydrazine reduction assay with Eu(II)-DTPA as a reductant was conducted for short times (2 min), high activity could be achieved because the Eu-DTPA was stable for only short times. Under these optimal conditions, the maximal specific activity for hydrazine reduction at 100 mM hydrazine was found to be 300 ± 15 nmol of NH₃ min⁻¹ (mg of MoFe

protein)⁻¹ for α -64^{Tyr→His}, 180 ± 3 nmol of NH_3 min⁻¹ (mg of MoFe protein)⁻¹ for β -98^{Tyr→His}, and 150 ± 2 nmol of NH_3 min⁻¹ (mg of MoFe protein)⁻¹ for β -99^{Phe→His}. These rates of hydrazine reduction compare to the rate of 320 nmol of NH_3 min⁻¹ (mg of MoFe protein)⁻¹ catalyzed by the wild-type MoFe protein with Fe protein as the electron donor.

For the β -98^{Tyr→His}, β -99^{Phe→His}, and α -64^{Tyr→His} MoFe protein variants, the rate of reduction of hydrazine was dependent on the concentration of Eu(II)-DTPA (Figure S2 of the Supporting Information), with saturation being approached above 1 mM Eu(II)-

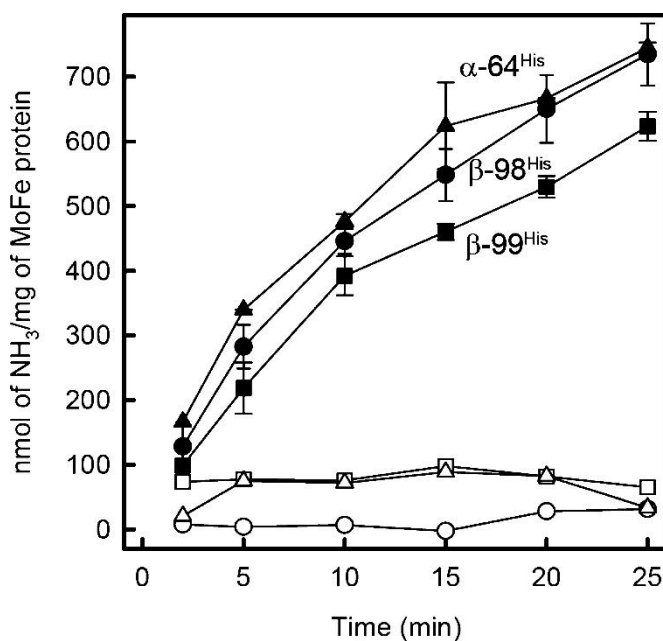


Figure 4-2. Fe protein-independent hydrazine reduction catalyzed by MoFe protein variants. Time course of the reduction of hydrazine to ammonia reported as nanomoles of ammonia formed per milligram of MoFe protein catalyzed by α -64^{His} (▲), β -98^{His} (●), or β -99^{His} (■) variant MoFe protein. The corresponding empty symbols are the no protein controls. These assays were performed with a final concentration of 1 mM Eu(II)-DTPA, 2.9 nmol of (1.83 μ M) MoFe protein, and 100 mM hydrazine at 25 °C. Bars represent the standard deviation for two measurements.

DTPA. These findings indicate that it is possible to saturate for the reductant and that there is a finite binding affinity.

In addition, the rates of hydrazine reduction were dependent on the concentration of hydrazine (Figure 4-3). Fits of the data to the Michaelis–Menten equation gave K_m values of ~ 48 mM for α -64^{Tyr→His}, 21 mM for β -98^{Tyr→His}, and 17 mM for β -99^{Phe→His}. V_{max} values were found to be ~ 490 nmol of $\text{NH}_3 \text{ min}^{-1} (\text{mg of MoFe protein})^{-1}$ for α -64^{Tyr→His}, 250 nmol

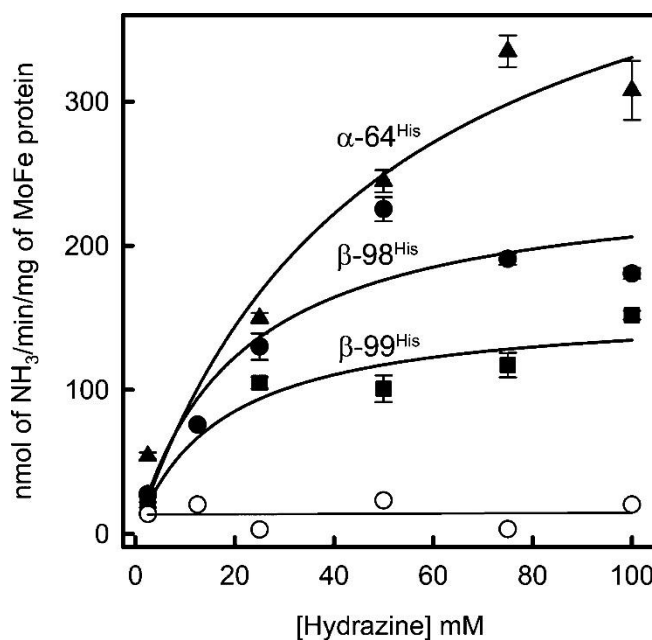


Figure 4-3. Concentration dependence of hydrazine on MoFe protein substrate

reduction. The nanomoles of ammonia per mg of MoFe protein for the α -64^{His} (\blacktriangle), β -98^{His} (\bullet), and β -99^{His} (\blacksquare) variants as a function of hydrazine concentration are shown. The empty symbol corresponds to a no protein background control. All assays were conducted for 2 min at 25 °C with a final concentration of 1 mM Eu(II) DTPA, 100 mM hydrazine, and 2.9 nmol of (1.83 μ M) MoFe protein. The data were fit to Michaelis–Menten equation (\square) using SigmaPlot with r^2 values of 0.94, 0.87, and 0.91 for the α -64^{His}, β -98^{His}, and β -99^{His} MoFe protein data, respectively.

of $\text{NH}_3 \text{ min}^{-1} (\text{mg of MoFe protein})^{-1}$ for $\beta\text{-98}^{\text{Tyr}\rightarrow\text{His}}$, and $160 \text{ nmol of NH}_3 \text{ min}^{-1} (\text{mg of MoFe protein})^{-1}$ for $\beta\text{-99}^{\text{Phe}\rightarrow\text{His}}$.

The $\beta\text{-98}^{\text{Tyr}\rightarrow\text{His}}$, $\beta\text{-99}^{\text{Phe}\rightarrow\text{His}}$, and $\alpha\text{-64}^{\text{Tyr}\rightarrow\text{His}}$ variant MoFe proteins were found to reduce azide (N_3^-) to ammonia (monitored) with Eu(II)-DTPA as the electron donor (Table 4-1). The reduction midpoint potential of Eu(II) can be modified by changing the polyaminocarboxylate ligand (DTPA, EGTA, or EDTA). The EuIII/II-DTPA, EuIII/II-EGTA, and EuIII/II EDTA redox couples have reduction potentials of -1.14 , -0.88 , and -0.84 V versus the normal H_2 electrode (NHE), respectively.¹⁶ All three ligand complexes with Eu(II) were examined with the three variant proteins for reduction of azide to ammonia (Table 4-1, Figure 4-S2). For some of the variants, the EGTA and EDTA complexes with Eu(II) showed higher rates of azide reduction. The Eu(II)-DTPA complex catalyzes proton reduction to form H_2 even in the absence of enzyme, whereas the Eu(II)-EDTA complex does not. This allowed the Eu(II)EDTA complex to be examined as a source of electrons for proton reduction to form H_2 for the three proteins. Only the $\beta\text{98}^{\text{Tyr}\rightarrow\text{His}}$ protein showed significant H_2 evolution rates above background.

Structural Characterization

The structure of the $\beta\text{98}^{\text{Tyr}\rightarrow\text{His}}$ MoFe protein was determined and refined to 1.97 \AA resolution and compared to the structure of the wild-type MoFe protein (PDB entry 3U7Q, 1.0 \AA)(Table 4-S1). Subtle structural differences were observed in the immediate vicinity of the amino acid substitution and in the solvent structure immediately around FeMo-co. Most notable with respect to the later is the $\sim 1.5 \text{ \AA}$ difference in the position of a water molecule coordinating homocitrate resulting from the differences in the H binding groups of Tyr and

His at position β -98 (Figure 4-4). The histidine residue in the variant refines in a slightly different orientation relative to the tyrosine in the wildtype MoFe protein and may be better poised for electron transfer due to the δ orbital dominance of this residue relative to the π orbital dominance of tyrosine. The change in side chain pK_a 's may also have an effect on the active site electrostatic environment and electron transfer pathway.

Table 4-1. Product Formation of MoFe Protein Variants Using Eu(II)-L as a Reductant^a

protein	hydrazine (nmol of NH ₃ /mg of MoFe protein)	azide (nmol of NH ₃ /mg of MoFe protein)			proton (nmol of H ₂ /mg of MoFe protein)
	Eu-DTPA	Eu-DTPA	Eu-EGTA	Eu- EDTA	Eu-EDTA
α -64 ^{His}	662 \pm 29	108 \pm 8	150 \pm 21	167 \pm 29	ND ^b
β -98 ^{His}	650 \pm 8	125 \pm 4	104 \pm 8	79 \pm 16	262 \pm 24
β -99 ^{His}	530 \pm 21	ND ^b	137 \pm 12	92 \pm 8	ND ^b

^aBoth the hydrazine and azide assays were conducted at 30 °C for 20 min, while the proton assays were conducted for 40 min at 30 °C. The hydrazine concentration was 100 mM and the azide concentration 10 mM. All assays were performed at pH 7.0. ^bNone detected.

Calculations on Normal-Mode Conformational Changes

The findings described above reveal that it is possible to create a MoFe protein through amino acid substitutions that can reduce a number of substrates without the Fe protein and ATP. This suggests that these substitutions might regulate electron transfer from the P cluster to FeMo-co and/or the reactivity of FeMo-co. The nature of these

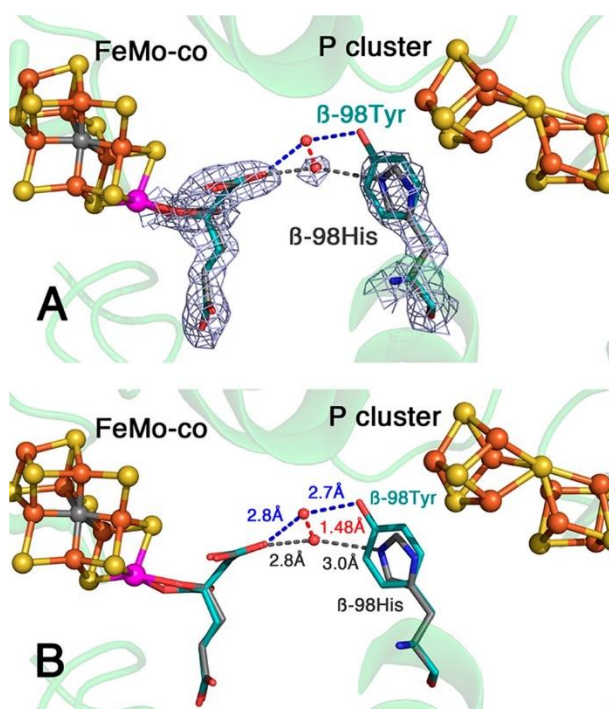


Figure 4-4. Crystal structure of the β -98^{Tyr→His} variant MoFe protein. (A) Shown is the experimental electron density superimposed with the wild-type MoFe protein (PDB entry 3U7Q). Subtle differences in structures between the two proteins are shown. (B) View of the β 98^{Tyr→His} variant structure superimposed with the wild-type structure (PDB entry 3U7Q), highlighting the change in the solvent structure adjacent to the FeMo cofactor.

conformational changes remains elusive, but the results from this work point to the possible participation of amino acids located between the P cluster and FeMo-co. To further explore the possible communication between the Fe protein and the MoFe protein, the vibrational normal modes that describe the large-amplitude motions of the nitrogenase complex were calculated according to a coarse-grained description of the proteins. A covariance analysis of the displacement of amino acid residues reveals a cross correlation between the motion of the two Fe proteins (Figure 4-S3), suggesting that the motion of one of the two Fe proteins causes a response in the region between the P cluster and FeMo-co. In particular, motion of residues α -64^{Tyr}, β -98^{Tyr}, and β -99^{Phe} in the MoFe protein correlates with the motion of the Fe protein. Figure 5 displays the correlation between these residues and the rest of the nitrogenase complex. As one can see, there is a trivial in-phase correlation between the motion of residues α -64^{Tyr}, β 98^{Tyr}, and β -99^{Phe} and the neighboring residues within the MoFe protein, which decays quickly in space. Remarkably, Figure 5 shows a high degree of out-of-phase correlation between these residues and the Fe proteins. The normal mode contributing most to this correlation corresponds to an out-of phase rolling motion of the Fe proteins on the surface of the MoFe protein (Figure 6). These results suggest a dynamic coupling between the motion of the Fe protein and the MoFe protein region lying between the P cluster and FeMo-co, which may provide the key to understand the unique role of the Fe protein in regulating activity within the MoFe protein necessary for electron transfer and substrate reduction. The predicted motions within the MoFe protein are especially interesting because of the lack of any observed changes in different X-ray structures determined to date.²⁷

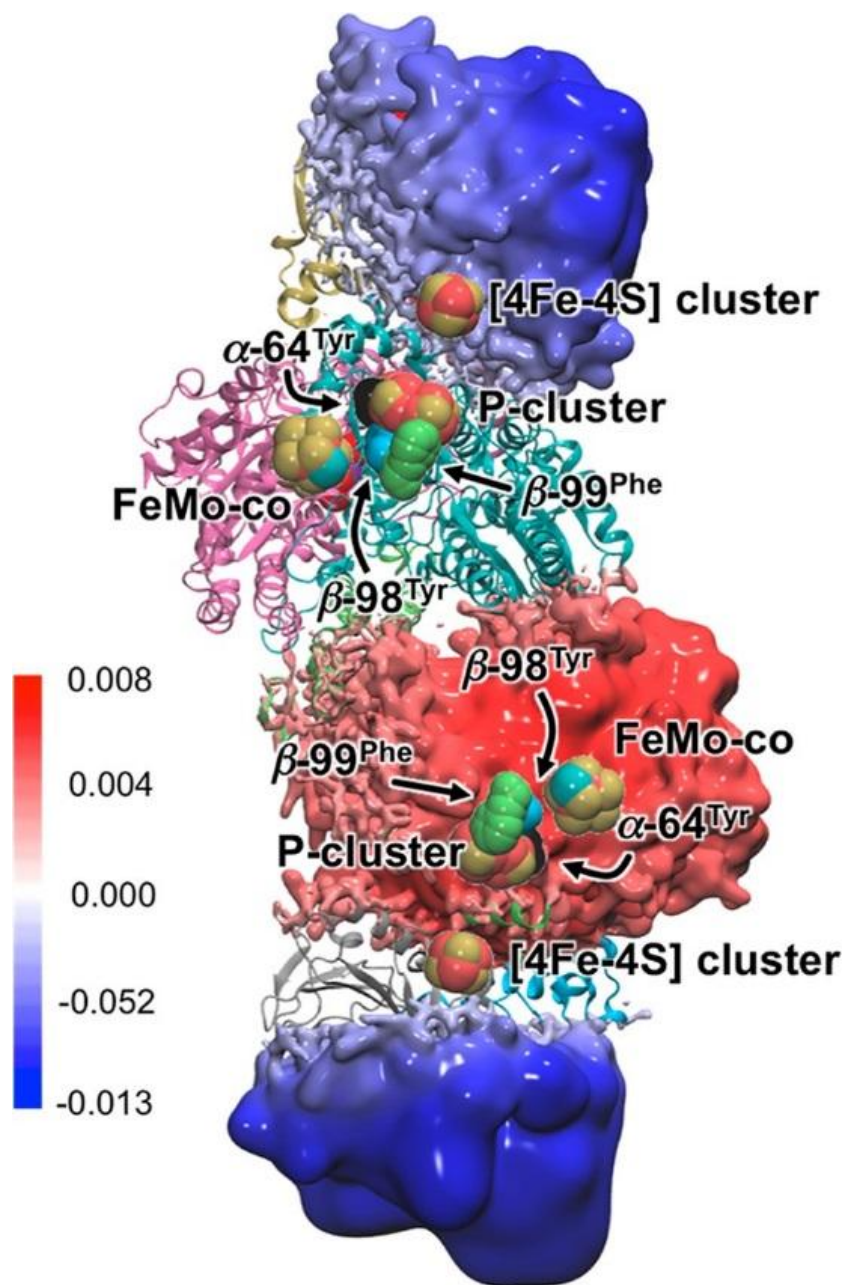


Figure 4-5. Mechanical coupling among residues α -64^{Tyr}, β -98^{Tyr}, and β 99^{Phe} of one of the two $\alpha\beta$ units and the rest of the MoFe protein-Fe protein complex. A similar coupling is present among the three residues.

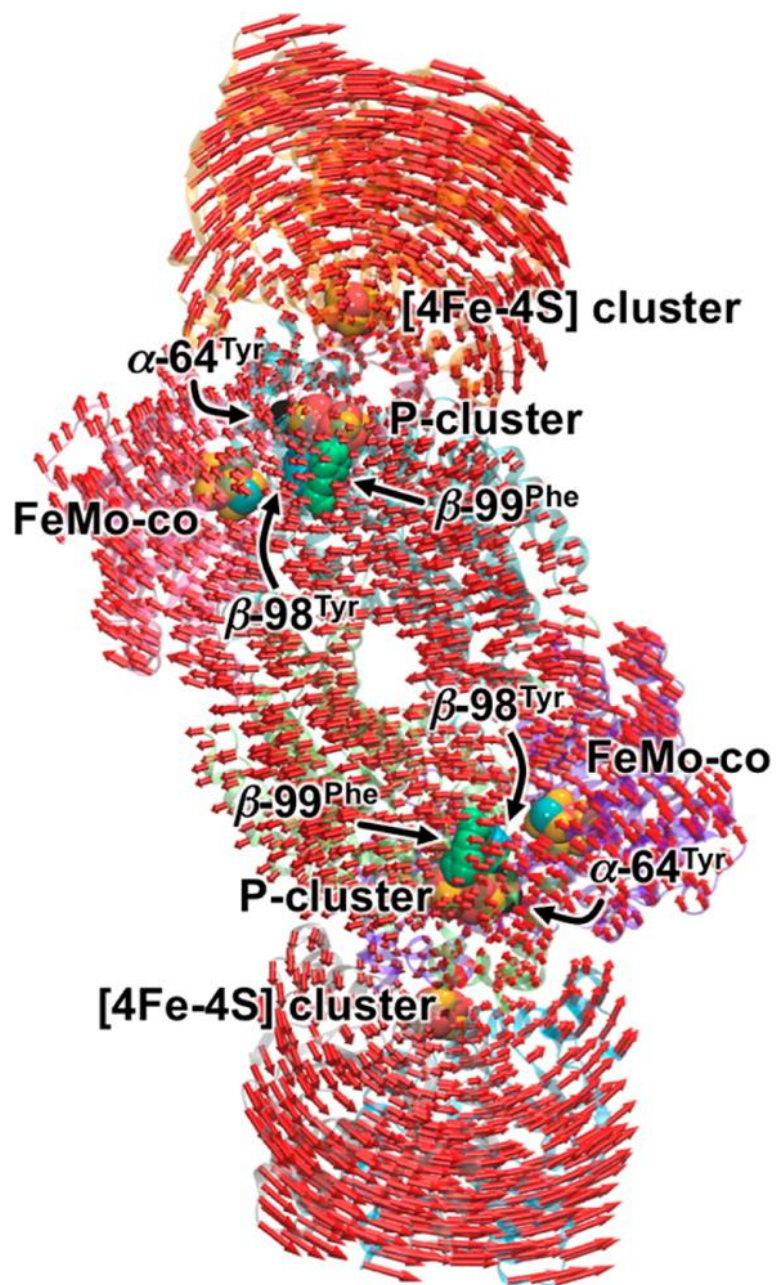


Figure 4-6. Collective motion corresponding to the rocking of the Fe protein on the MoFe protein surface. The length of the arrows is proportional to the displacement of the amino acid residues. The locations of the metal clusters and α -64^{Tyr}, β -98^{Tyr}, and β -99^{Phe} residues are shown.

Conclusions

Nitrogenase is a dynamic protein, with protein conformational changes playing key roles at various steps in the catalytic cycle.²⁷⁻³⁰ The absolute need for the Fe protein and ATP binding to the MoFe protein to support N₂ reduction suggests that the protein-protein association communicates conformational changes within the MoFe protein essential to some aspects of catalysis, perhaps intramolecular electron transfer of the other subunit and the rest of the complex. Regions of correlation and anticorrelation are enclosed by red and blue surfaces, respectively. The extent and color scale of the surfaces correspond to the average of the values of covariance matrix elements (in square angstroms) for the three residues. The locations of the metal clusters and α -64^{Tyr}, β -98^{Tyr}, and β -99^{Phe} residues are shown. (i.e., initiation of deficit spending electron transfer) and/or substrate binding and reduction. The results presented here add to the earlier finding that substitution of amino acids buried deep within the MoFe protein located between the P cluster and FeMo-co can create a MoFe protein that is able to reduce a number of substrates without the Fe protein and ATP. The structure of the β -98^{Tyr→His} variant reveals no global structural differences compared to the wild-type structure, with small changes localized near the amino acid substitution and homocitrate-coordinated bound water. The structure reveals only subtle differences in structure of the protein surrounding FeMo-co. This small shift coupled with the chemical difference in the amino acid side chains of tyrosine and histidine is sufficient to significantly alter the reactivity of the MoFe protein. This data suggests that equally subtle changes might be sufficient to activate electron transfer when the Fe protein binds. Finally, computational normal-mode analysis reveals that the Fe protein and this region of the MoFe protein are

connected in terms of molecular motion, suggesting a mechanism for how Fe protein might communicate into the MoFe protein to affect activity.

REFERENCES

- (1) Burgess B. K., Lowe D. J. (1996) *Chem. Rev.* 96, 2983–3012.
- (2) Yang Z. Y., Danyal K., Seefeldt L. C. (2011) *Methods Mol. Biol.* 766, 9–29.
- (3) Spatzal T., Aksoyoglu M., Zhang L., Andrade S. L. A., Schleicher E., Weber S., Rees D. C., Einsle O. (2011) *Science* 334, 940.
- (4) Einsle O., Tezcan F. A., Andrade S. L. A., Schmid B., Yoshida M., Howard J. B., Rees D. C. (2002) *Science* 297, 1696–1700.
- (5) Georgiadis M. M., Komiya H., Chakrabarti P., Woo D., Kornuc J. J., Rees D. C. (1992) *Science* 257, 1653–1659.
- (6) Hageman R. V., Burris R. H. (1978) *Proc. Natl. Acad. Sci. U.S.A.* 75, 2699–2702.
- (7) Duval S., Danyal K., Shaw S., Lytle A. K., Dean D. R., Hoffman B. M., Antony E., Seefeldt L. C. (2013) *Proc. Natl. Acad. Sci. U.S.A.* 110, 16414–16419.
- (8) Danyal K., Dean D. R., Hoffman B. M., Seefeldt L. C. (2011) *Biochemistry* 50, 9255–9263.
- (9) Lowe D. J., Ashby G. A., Brune M., Knights H., Webb M. R., Thorneley R. N. F. (1995) ATP hydrolysis and energy transduction by nitrogenase. In *Nitrogen Fixation: Fundamentals and Applications* pp 103–108, Springer, Dordrecht, The Netherlands.
- (10) Shah V. K., Stacey G., Brill W. J. (1983) *J. Biol. Chem.* 258, 12064–12068.
- (11) Roth L. E., Nguyen J. C., Tezcan F. A. (2010) *J. Am. Chem. Soc.* 132, 13672–13674.
- (12) Roth L. E., Tezcan F. A. (2012) *J. Am. Chem. Soc.* 134, 8416–8419.
- (13) Danyal K., Inglet B. S., Vincent K. A., Barney B. M., Hoffman B. M., Armstrong F. A., Dean D. R., Seefeldt L. C. (2010) *J. Am. Chem. Soc.* 132, 13197–13199.
- (14) Christiansen J., Goodwin P. J., Lanzilotta W. N., Seefeldt L. C., Dean D. R. (1998) *Biochemistry* 37, 12611–12623.

- (15) Corbin J. L. (1984) *Appl. Environ. Microbiol.* 47, 1027–1030.
- (16) Vincent K. A., Tilley G. J., Quammie N. C., Streeter I., Burgess B. K., Cheesman M. R., Armstrong F. A. (2003) *Chem. Commun.*, 2590–2591.
- (17) Ng J. D., Gavira J. A., García-Ruíz J. M. (2003) *J. Struct. Biol.* 142, 218–231.
- (18) Georgiadis M. M., Komiya H., Chakrabarti P., Woo D., Kornuc J. J., Rees D. C. (1992) *Science* 257, 1653–1659.
- (19) Sarma R., Barney B. M., Keable S., Dean D. R., Seefeldt L. C., Peters J. W. (2010) *Inorg. Biochem.* 104, 385–389.
- (20) Otwinowski Z., Minor W. (1997) Processing of X-ray diffraction data collected in oscillation mode. In *Methods in Enzymology* (Charles, W., and Carter, J., Eds.) pp 307–326, Academic Press, New York.
- (21) Winn M. D., Ballard C. C., Cowtan K. D., Dodson E. J., Emsley P., Evans P. R., Keegan R., Krissinel E. B., Leslie A. G., McCoy A., McNicholas S. J., Murshudov G. N., Pannu N. S., Potterton E. A., Powell H. R., Read R. J., Vagin A., Wilson K. S. (2011) *Acta Crystallogr. D* 67, 235–242.
- (22) Murshudov G. N., Vagin A. A., Dodson E. J. (1997) *Acta Crystallogr. D* 53, 240–255.
- (23) Tirion M. M. (1996) *Phys. Rev. Lett.* 77, 1905–1908.
- (24) Atilgan A. R., Durell S. R., Jernigan R. L., Demirel M. C., Keskin O., Bahar I. (2001) *Biophys. J.* 80, 505–515.
- (25) Leioatts N., Romo T. D., Grossfield A. (2012) *J. Chem. Theory Comput.* 8, 2424–2434.
- (26) Balabin I. A., Yang W., Beratan D. N. (2009), *Proc. Natl. Acad. Sci. U.S.A.* 106, 14253–14258.

- (27) Tezcan F. A., Kaiser J. T., Mustafi D., Walton M. Y., Howard J. B., Rees D. C. (2005) *Science* 309, 1377–1380.
- (28) Danyal K., Mayweather D., Dean D. R., Seefeldt L. C., Hoffman B. M. (2010) *J. Am. Chem. Soc.* 132, 6894–6895.
- (29) Tezcan F. A., J. T. Kaiser, Howard J. B., Rees D. C. (2015) *J. Am. Chem. Soc.* 137, 146–149.
- (30) Mayweather D., Danyal K., Dean D. R., Seefeldt L. C., Hoffman B. M. (2012) *Biochemistry* 51, 8391–8398.

Supporting Information

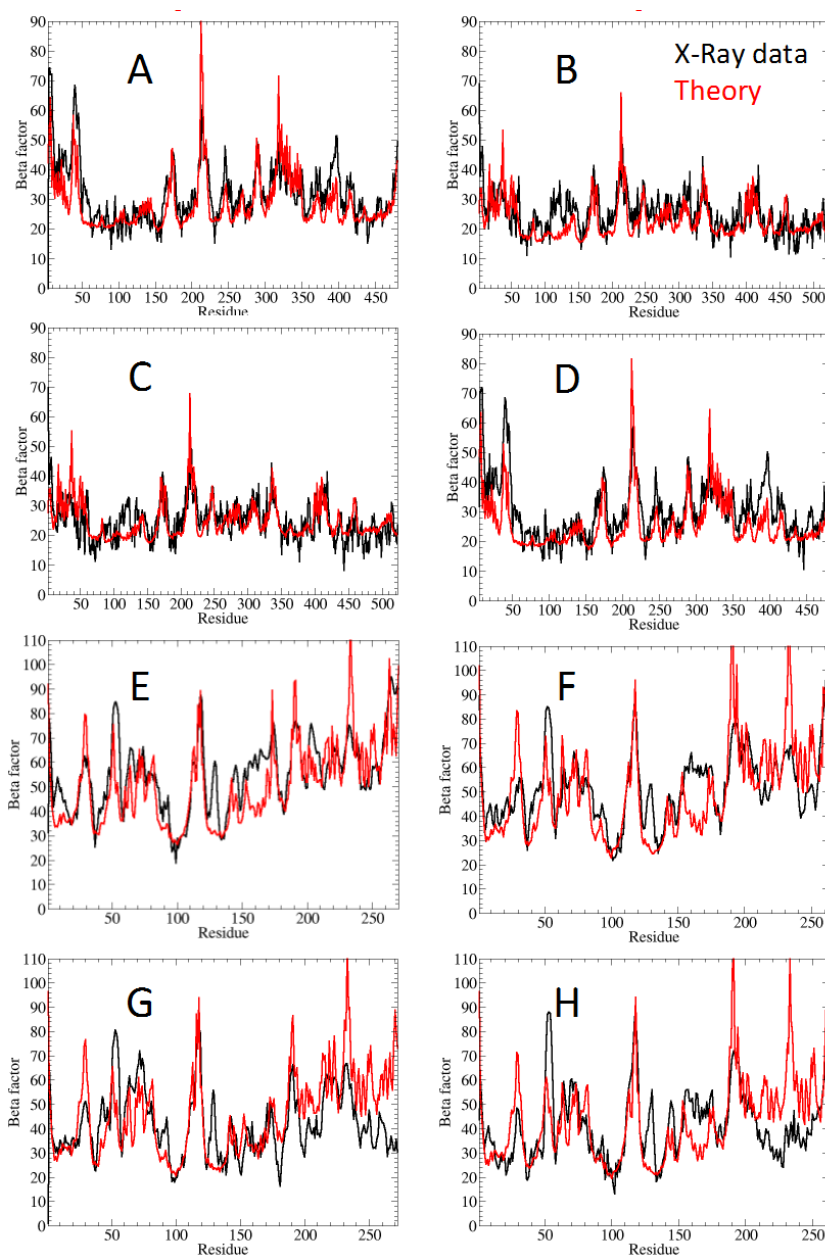


Figure 4-S1. Beta factors for the nitrogenase complex. Comparison between the crystallographic (black line) and calculated (red line) beta factors (in \AA^2) for the Fe protein/MoFe protein complex (crystal structure 2AFK). For sake of clarity, the beta factors are reported separately for each subunit (see **Figure 4-1**).

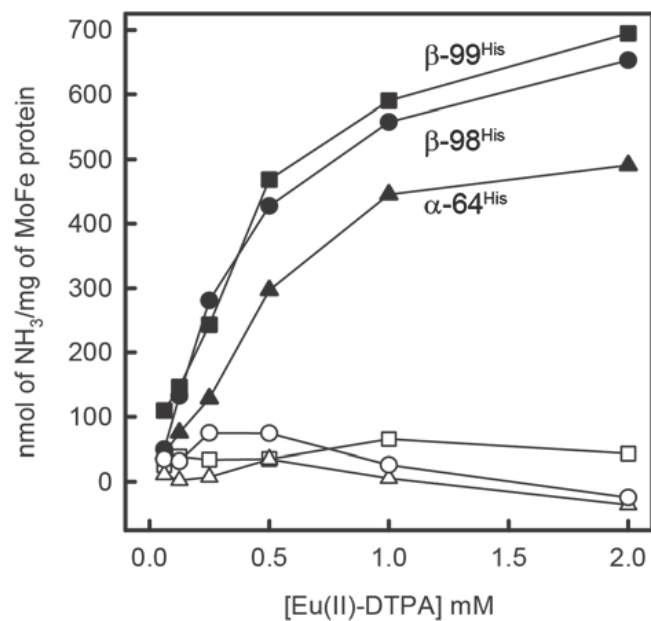


Figure 4-S2. Concentration dependence of Eu (II)-DTPA on MoFe protein substrate reduction. The nmol of ammonia formed per mg MoFe protein is shown as a function of the concentration of Eu(II)-DTPA for the α -64His (\blacktriangle), β -98His (\bullet), and β -99His (\blacksquare) MoFe proteins. The corresponding open symbols are the no protein controls. All assays were conducted for 20 min with a final concentration of 100 mM hydrazine and 2.9 nmol (1.83 μ M) of MoFe protein at 25°C.

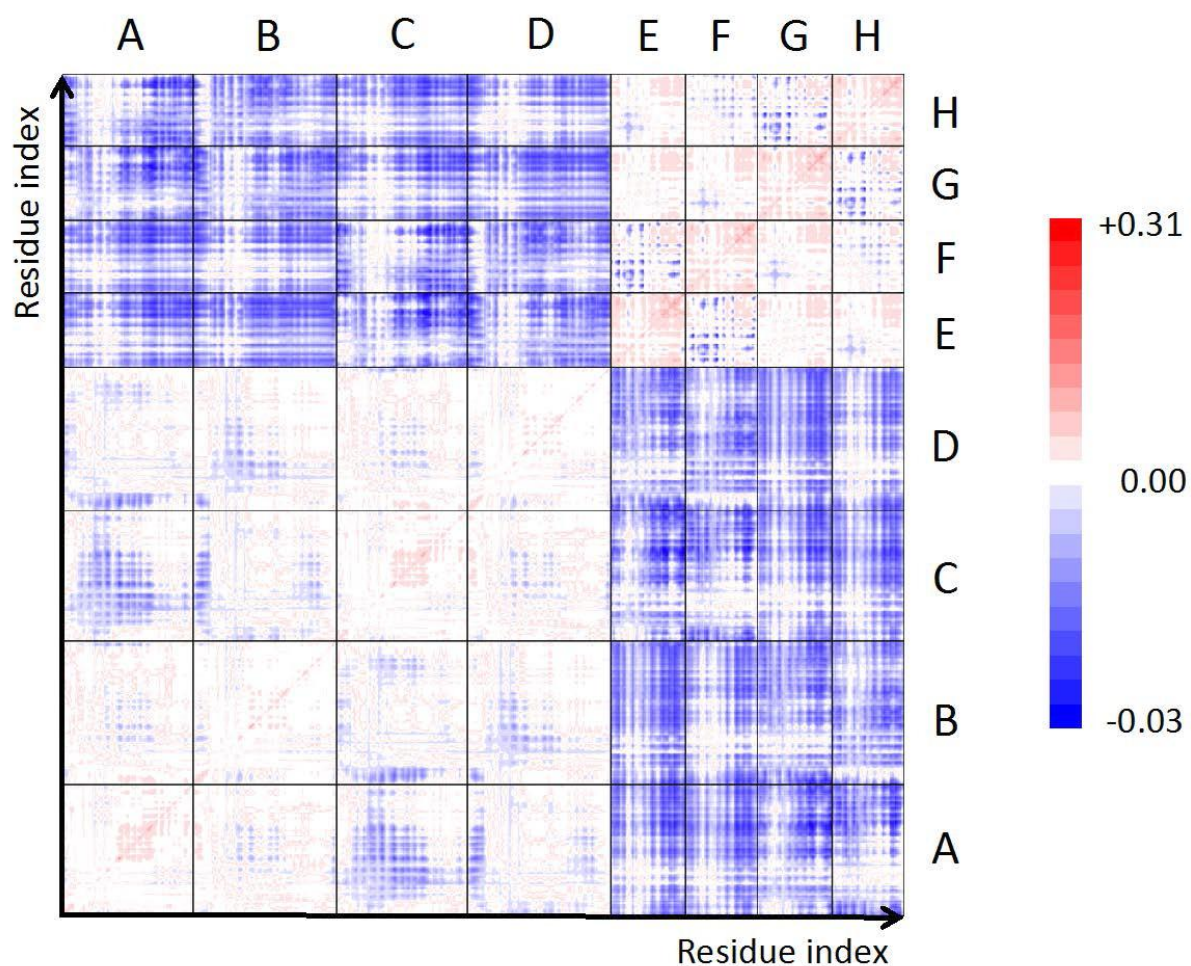


Figure 4-S3. Covariance analysis. Covariance matrix (in \AA^2) for the MoFe protein/Fe protein complex. For sake of clarity, the matrix is divided into quadrants corresponding to the various possible subunit pairs (see **Figure 4-1**). Regions of correlated (in-phase) and anti-correlated (out-of-phase) motions are shown in red and blue, respectively.

Table 4-S1: Data Statistics for β -98^{Tyr→His} MoFe Protein Structure

cell dimensions	$a = 80.80 \text{ \AA}$ $b = 130.83 \text{ \AA}$ $c = 108.11 \text{ \AA}$ $\alpha = \gamma = 90.00^\circ$ $\square\square\square\square 111.14$
space group	$P2_1$
wavelength	$\lambda_1 = 0.97947$
resolution(\AA)	35-1.97
completeness (%)	96.39 (84.1) ^D
obsd reflections	134339
unique reflections	127252
Avg redundancy	3.5
I/σ	2.5 (25.7) ^D
$R_{\text{sym}}(\%)$	8.0 (37.6) ^D
Refinement Statistics	
Resolution (\AA)	35-1.97
R_{cryst}	21.5
R_{free}^c (%)	26.3
Real Space CC^a (%)	94.5
Mean B Value (overall; \AA)	41.8
Coordinate Error (based on maximum likelihood, RMSD from ideality:	0.15
Bonds (\AA)	0.02
Angles ($^\circ$)	2.92
Ramchandran Plot ^e :	
Most favored (%)	95.6
Additional allowed (%)	4.2
Outliers (%)	0.20

^bNumbers in parenthesis refer to the highest resolution shell. ^c $R_{\text{sym}} = 100 * \frac{\sum_h \sum_i |I_i(h) - \langle I(h) \rangle|}{\sum_h I(h)}$ where $I_i(h)$ is the i^{th} measurement of reflection h and $\langle I(h) \rangle$ is the average value of the reflection intensity. ^e $R_{\text{cryst}} = \frac{\sum ||F_o| - |F_c||}{\sum |F_o|}$ where F_o and F_c are the observed and calculated structure factor

CHAPTER 5

CHARACTERIZATION AND MODULATION OF THE ISOLATED IRON
MOLYBDENUM COFACTOR**Abstract**

The biological fixation of atmospheric N_2 to form ammonia for use in microbes is accomplished by the enzyme nitrogenase. The molybdenum nitrogenase is the most common of these, and it contains at its active the FeMo-cofactor a complex metal cluster with the composition $[7Fe-9S-C-Mo-homocitrate]$.¹ Nitrogenase is a two component protein, the iron protein (Fe protein) and the molybdenum iron protein (MoFe protein). The Fe protein delivers electrons to the MoFe protein in a sequential manner, hydrolyzing 2 MgATP per electron transferred.² The FeMo-cofactor in the MoFe protein is where substrate binding and reduction occurs. The MoFe protein can perform reductive chemistry on a wide variety of substrates other than nitrogen. For example, nitrogenase can reduce cyanide to methane and ammonia. Nitrogenase is also able to reduce azide to ammonia, hydrazine, and nitrogen, as well as acetylene to ethylene, and protons to hydrogen.^{2,3} Along with these, there are many variants of nitrogenase that are able to reduce an even wider variety of substrates, such as carbon dioxide to methane.⁴

The FeMo-cofactor can be extracted from nitrogenase and isolated into an organic solvent, most commonly *N*-methyl formamide (NMF), and has been shown to activate nitrogenase enzymes in which a mutation in the organism prevents the synthesis of FeMo-co.⁵ In nitrogenase FeMo-co is bound to the protein via a histidine to the molybdenum atom of FeMo-co and a cysteine to the capping iron atom.² It appears that when the cofactor is

extracted in NMF, both of these sites become ligated to molecules of NMF.¹ It has been shown that thiols bind with high affinity in a fashion that sharpens up the EPR spectrum of isolated FeMo-co, making it appear much like that of the protein bound FeMo-co signal. The interaction has been quantified and shows one thiol binding per FeMo-co.⁶

Substrate binding assays have been performed on FeMo-co. Evidence for cyanide (CN⁻) binding implies that FeMo-co binds one CN⁻ tightly with a second cyanide CN⁻ loosely associated to the metal cluster.⁷ Interestingly FeMo-co has also been shown to bind carbon monoxide (CO⁻), though only upon reduction at a glassy carbon electrode to a potential of roughly -0.85 volts vs. SCE. This is interesting in that it shows that the isolated cofactor can be poised in ways that are not possible in the protein.⁸

More recent studies have shown the isolated cofactor perform catalytic reduction of various substrates. Isolated FeMo-cofactor in NMF on a glassy carbon electrode was able to reduce protons to form hydrogen gas.⁹ FeMo-co which after isolation was placed in an aqueous buffered solution in the presence of various low potential chemical reductants and was shown to reduce CO⁻, CN⁻, and CO², reducing the nitrogen to ammonia, the carbons to methane and other hydrocarbons, though the turnover number was distressingly low, in some cases not even achieving one.^{10, 11}

These are very exciting results as now there is an assay that can be performed and used to probe reactivity the isolated cofactor, and to understand which conditions can alter this activity.

Experimental Procedures

All chemicals were purchased from Sigma-Aldrich (St. Louis, MO) or Fischer Scientific (Fair Lawn, NJ) and were used without further purification. Wild type MoFe protein from *Azotobacter vinelandii* was purified under strict anaerobic conditions with slight modifications to previously described protocols.¹³ All proteins were obtained at greater than 95% purity as judged by SDS-PAGE analysis using Coomassie blue staining and demonstrated full specific activity (greater than 2,000 nmolH₂/min/mg protein). Handling of proteins was done in septum-sealed serum vials under an argon atmosphere. All transfers of gases and liquids were done using gastight syringes.

Extraction of the Cofactor: Isolated FeMo-co was extracted using the on column extraction method described previously.¹² In short; purified MoFe protein is loaded on a DE-52 anion exchange column and rinsed with several column volumes on NMF to remove all water. The protein is completely denatured under these conditions after 10 minutes. An NMF solution containing 500 mM of the organic salt (Bu)₄NCl is then used to elute the FeMo-cofactor molecule. This typically extracts 60-80% of the cofactor and gives a Mo to Fe ratio of roughly 1:8, demonstrating that little, if any contaminating P cluster comes across with the FeMo-co.

Determination of Cofactor Concentration: FeMo-co concentration was determined in one of two ways. The first was by determining the Mo and Fe concentrations in the extracted solution, and assuming one atom of Mo per FeMo-co. This was done by either ICPMS, or a colorimetric assay on a denatured sample that had been treated with the appropriate ligands. Once we had determined the concentration using one of the above methods a UV/Vis spectra

was taken that was used to determine the extinction coefficients of FeMo-co in NMF for future determination of FeMo-co. (Table 5-1)

Methane and Hydrogen production Assays: Assays using CO₂ as substrate were conducted in 9.4-mL serum vials containing 1.0 ml of an assay buffer consisting of 150 mM Tris at pH 8.0 and N-Methylformamide. The reductant was prepared fresh by mixing a solution of 1 M Eu(II)Cl₂ in anaerobic 150 mM Tris/HCl at pH 8.0 at a 1:1 ratio with a 1 M stock of one of the three following ligands dissolved in anaerobic 150 mM Tris/HCl pH 8.0; diethylenetriaminepentaacetic acid (DTPA), ethyleneglycoltetraacetic acid (*EGTA*), or ethylenediaminetetraacetic acid (EDTA). After degassing the assay buffer sodium bicarbonate was added to the serum vials and allowed to equilibrate with the solution for 20 minutes, then Eu(II)-Ligand was added to the serum vial. The assay vials were then ventilated to atmospheric pressure and 1.5 nmol FeMo-cofactor was quickly added to initiate the reaction. The samples were then incubated at 30°C and shaken at 150 RPM in a water bath shaker. Methane (CH₄) was quantified via gas chromatography by injection of 200 µL of the gas phase of the reaction vial into a Shimadzu GC-8A equipped with a flame ionization detector fitted with a 30 cm × 0.3 cm Porapak N column with nitrogen as the carrier gas. The injection/detection temperature was set to 180 °C, and the column temperature was set to 110 °C. The standard curves with high linearity were created by using methane gas diluted with argon in 9.4-mL serum vials. Hydrogen (H₂) was quantified by gas chromatography by injection of 40 µL of the gas phase of the reaction vial into a Shimadzu GC-8A equipped with a thermal conductivity detector fitted with a 6 ft x 2.1 mm Supelco 60/80 Mol Sieve 5a column with argon as the carrier gas. The injection/detection

temperature was set to 100 °C, and the column temperature was set to 50 °C. The standard curves with high linearity were created by using hydrogen gas diluted with argon in 9.4-mL serum vials.

Hydrazine and Azide Assays: Assays done with the nitrogenous substrates N_2H_4 and N_3^- were conducted under the same conditions above, except where noted. The substrates, N_2H_4 and NaN_3 , were dissolved in a Tris HCl solution whereafter the pH was adjusted to pH 8.0 prior to degassing. The samples were then incubated at 30°C and shaken at 150 RPM in a water bath shaker. Samples of 10 μL of the reaction solution were taken at the given reaction times. NH_3 was quantified using a fluorometric method with *o*-phthalaldehyde and mercaptoethanol as described previously on a Spex Fluorolog 3 spectrofluorimeter.¹⁴ The standard curve was created simultaneous to every assay using NH_4Cl at different concentrations.

Table 5-1: Extinction Coefficients of Isolated FeMo-co in NMF.

Wavelength (nm)	Extinction Coefficient mM-1cm-1
450	22.67
500	16.45
550	13.18
600	11.12
650	9.45
700	7.65

Results

The Reduction of carbon dioxide to methane using FeMo-cofactor with Eu(II)-DTPA as a reductant was achieved, and these results were optimized by adjusting NMF concentration in the buffer as well as adjusting the concentration of reductant present in the buffer to achieve a final activity of 69 nmol CH₄ per nmol FeMo-co per hour. (Fig 5-1) It was seen that increasing the concentration of reductant from 5mM to 75mM favored the reduction of CO₂ to CH₄. It was also seen that having a more organic solvent favors the reduction of CO₂, while having no effect on the nitrogenous substrate hydrazine (N₂H₄). (Fig 5-2)

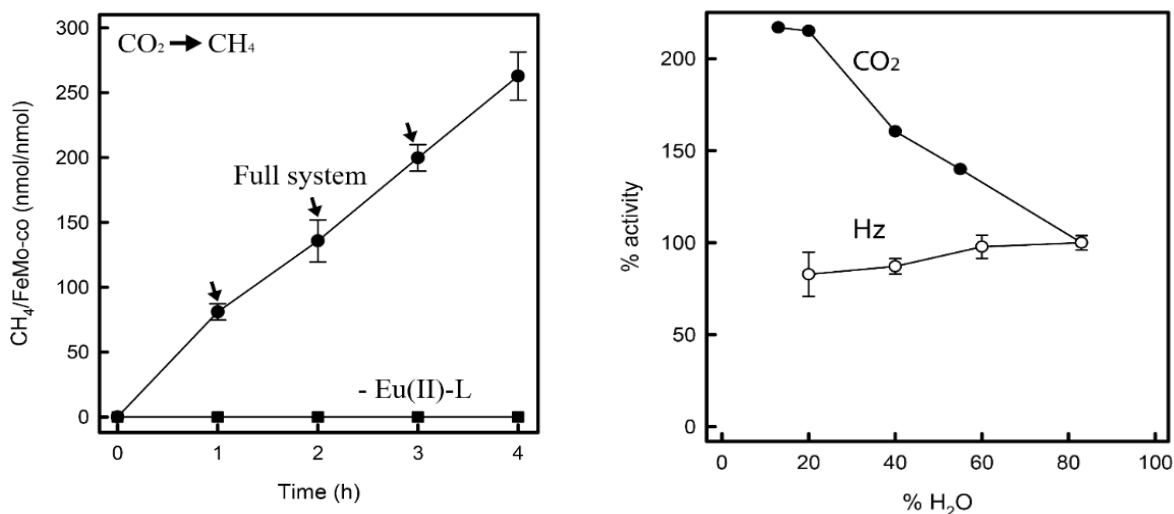


Figure 5-1. Reduction of Carbon Dioxide to Methane and the Effect of Solvent on

Activity. All assays were conducted at 30°C with 1.5 nmol of FeMo-co in a 1.5mL solution containing 150mM TRIS pH 8.0, NMF and 75mM Eu(II)-DTPA. (left) Time course showing the addition of further reductant at the designated times maintains the reaction. (right) Effect of reducing the water in the solvent on substrate reduction.

While only the lowest potential reductant, Eu(II)-DTPA (-1.15 V vs. SHE), was shown to reduce CO₂, and that only at high concentrations, FeMo-cofactor was able to reduce N₂H₄ with the much milder reductants Eu(II)-EGTA (-0.88 V vs. SHE) and Eu(II)-EDTA (0.84 V vs. SHE). Indeed, the reduction of hydrazine to ammonia was more efficient with the milder reductants and at a lower concentration of 5mM reductant.(Fig 5-3) Hydrazine was reduced at a rate of 40 nmol NH₃ per nmol FeMo-co per hour. An assay was conducted at varying concentration of hydrazine, but the assay was only conducted down to 5 mM hydrazine, and this was already saturated for substrate. The final substrate observed was

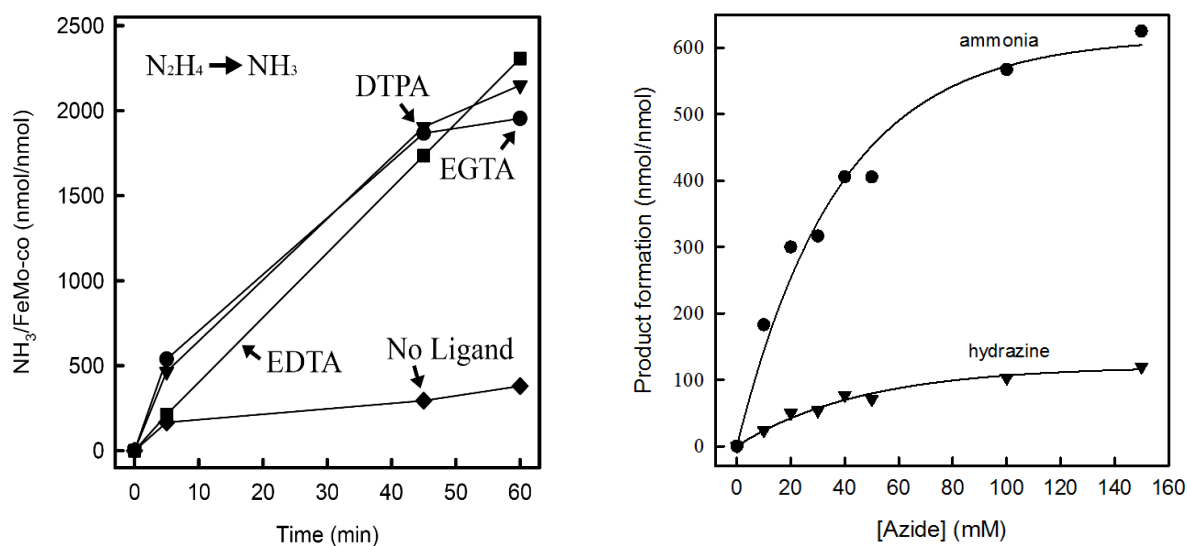


Figure 5-3. Reduction of Nitrogen Containing Substrates. All assays were conducted with 4.5 nmols of FeMo-co in a 1.5 ml solution containing 150mM TRIS pH 8.0, 250 μ L NMF, and 5 mM Eu(II)-L (left) Effect of changing the Eu(II)-L on hydrazine reduction (\bullet DTPA, \blacktriangledown EGTA, \blacksquare EDTA, and \blacklozenge no Ligand). (Right) Azide concentration dependence fit to the Michaelis-Menten equation. (\bullet NH₃, \blacktriangledown N₂H₄).

azide, which was reduced to ammonia and hydrazine. (Fig 5-4) A 30 minute assay with varying concentration on azide was performed and the data was fit to the Michaelis-Menten equation. The K_M for azide reduction was calculated to be 22 mM and the V_{max} was 20 nmol NH_3 and 4nmol N_2H_4 per nmol FeMo-co per min. This is deceptive as it has already been shown that hydrazine is a substrate of FeMo-co as well as a product so is likely being consumed in this reaction. (Fig 5-4)

Conclusions

The data collected using the Eu(II)-L chemical reductant as an electron donor to the isolated iron molybdenum cofactor yields some exciting results. First, this data shows a truly catalytic turnover of CO_2 , rather than the anemic reduction seen previously, proving that it is truly a catalytic reaction. Other substrates have also been identified as candidates for FeMo-co reduction. The most interesting data comes in the form of how these activities were achieved.

The makeup of the solvent had a large effect on substrate reduction. In order to achieve reduction of CO_2 at significant rates, the concentration of water had to be drastically reduced. The final composition of the buffer was less than 20% water, while this had little effect on hydrazine or azide reduction, and this had an inhibitory effect on hydrogen formation. Also of interest was the fact that adding a thiol ligand, benzene thiol, had the effect of reducing the activity of FeMo-co toward all substrates except azide. The reduction of CO_2 , N_2H_4 , and H^+ , were reduced by nearly 30% while azide reduction remained stable.

This is exciting as it shows that the activity of the FeMo-cofactor can be regulated and modulated to focus on reducing a substrate of interest by the simple expedient of adding

a ligand that will interact with the cofactor. This is seen in two ways as it is thought that NMF interacts with the cofactor as a ligand, and the increasing concentration of NMF in solution can change the way FeMo-co behaves, as well as the evidence provided by the addition of benzene-thiol, which coordinates with the capping Fe of FeMo-cofactor.

Further work into exploring various ligands that can coordinate with FeMo-co should be undertaken to better understand the effect these interactions have on the FeMo-cofactor.

REFERENCES

- (1) Lancaster K. M., Roemelt M., Ethenhuber P., Hu Y., Ribbe M. W., Neese F., Bergmann U., DeBeer S. (2011) *Science*. 334, 974-977.
- (2) Seefeldt L. C., Hoffman B. M., Dean D. R. (2009) *Annu. Rev. Biochem.* 78, 701-722.
- (3) Howard J. B., Rees D. C. (1996) *Chem Review*, 96, 2965.
- (4) Yang Z., Dean D. R., Seefeldt L. C. (2011) *J. Biol. Chem.* 286, 19417-19421.
- (5) Shah V. K., Brill W. (1977) *Proc. Natl. Acad. Sci.* 74, 3249.
- (6) Walters M. A., Chapman S. K., Orme-Johnson W. H. (1986) *Polyhedron*. 5, 561.
- (7) Smith B. E., Durant M. C., Airburst S. A., Gormal C. A., Gruenberg K. L. C., Henderson R. A., Ibrahim S. K., Le Gall T., Pickett C. J. (1999) *Coordination Chemistry Reviews*. 185, 669-687.
- (8) Ibrahim S. K., Vincent K., Gormal C. A., Smith B. E., Best A. P., Pickett C. J. (1999) *ChemComm*. 11, 1019-1020.
- (9) Ga T. L., Ibrahim S. K., Gormal C. A., Smith B. E., Pickett C. J. (1999) *ChemComm*. 9, 773-774.
- (10) Lee C. C., Hu Y., Ribbe M. W. (2012) *Angewandte Chemie*. 5451, 1947-1949.
- (11) Lee C. C., Hu Y., Ribbe M. W. (2015) *Angewandte Chemie*. 54, 1219-1222.
- (12) McLean P. A., Wink D. A., Chapman S. K., Hickman A. B., McKillop D. M., Orme-Johnson W. H. (1989) *Biochemistry*. 28, 9402-9406.
- (13) Christiansen J., Goodwin P. J., Lanzilotta W. N., Seefeldt L. C., Dean D. R. (1998) *Biochemistry*. 37, 12611-12623.
- (14) Taylor S., Ninjoor V., Dowd D. M., Tappel A. L. (1974) *Anal. Biochem.* 60, 153-162.

CHAPTER 6

SUMMARY

Summary

The work in this thesis has focused on two general aspects of the nitrogenase enzyme. The first is regulation and transfer of electrons from the Fe protein into and through the MoFe protein (Chapters 2-4). Second, understanding how the isolated FeMo-cofactor behaves outside of its natural environment was explored along with studies which begin to understand how to regulate substrate specificity of the isolated cofactor (Chapter 5).

The understanding of the conformational changes that occur upon formation of the MoFe:Fe complex have been expanded to include conformational gating steps that occur before both the ATP hydrolysis and the phosphate release steps of the Fe cycle. This study shows two distinct steps that take place sequentially; one directly before the ATP hydrolysis step, followed immediately by a second step before the phosphate release event occurs (Chapter 2). A novel technique has been developed which can be used to explore redox active crystals via poisoning the environment of the crystal at a given redox potential. This technique was used to visualize the biologically important P^{+1} state of the P cluster through X-ray crystallography, showing a novel structure with important mechanistic implications. The structural changes induced upon the binding of Fe protein likely cause a transient association of the β -188^{ser} of the MoFe protein to the P cluster, triggering an electron transfer event from the P cluster to the FeMo-cofactor (Chapter 3). Electron transfer from the P cluster to FeMo-co is regulated by the amino acid residues between these two metal cofactors, and three variant nitrogenases have been identified that allow electron transfer to

the FeMo-cofactor using chemical intermediates. The X-ray crystallographic structure of one of these variants has been visualized. This structure shows subtle changes in the solvent structure around the metal clusters, which allow the transfer of electrons to occur without the necessary binding of Fe protein to trigger this event (Chapter 4). The iron molybdenum cofactor, when isolated into NMF, can perform catalytic reduction of many substrates. Interestingly, varying the ligands coordinated to the FeMo-cofactor can regulate the substrate specificity and activity of the cofactor, and modulation of the activity of the isolated cofactor was achieved.

APPENDICIES

Appendix A: American Chemical Society's Policy on Thesis and Dissertations

American Chemical Society's Policy on Theses and Dissertations

If your university requires you to obtain permission, you must use the RightsLink permission system.
See RightsLink instructions at <http://pubs.acs.org/page/copyright/permissions.html>.

This is regarding request for permission to include **your** paper(s) or portions of text from **your** paper(s) in your thesis. Permission is now automatically granted; please pay special attention to the **implications** paragraph below. The Copyright Subcommittee of the Joint Board/Council Committees on Publications approved the following:

Copyright permission for published and submitted material from theses and dissertations

ACS extends blanket permission to students to include in their theses and dissertations their own articles, or portions thereof, that have been published in ACS journals or submitted to ACS journals for publication, provided that the ACS copyright credit line is noted on the appropriate page(s).

Publishing **implications** of electronic publication of theses and dissertation material

Students and their mentors should be aware that posting of theses and dissertation material on the Web prior to submission of material from that thesis or dissertation to an ACS journal may affect publication in that journal. Whether Web posting is considered prior publication may be evaluated on a case-by-case basis by the journal's editor. If an ACS journal editor considers Web posting to be "prior publication", the paper will not be accepted for publication in that journal. If you intend to submit your unpublished paper to ACS for publication, check with the appropriate editor prior to posting your manuscript electronically.

Reuse/Republication of the Entire Work in Theses or Collections: Authors may reuse all or part of the Submitted, Accepted or Published Work in a thesis or dissertation that the author writes and is required to submit to satisfy the criteria of degree-granting institutions. Such reuse is permitted subject to the ACS' "Ethical Guidelines to Publication of Chemical Research" (<http://pubs.acs.org/page/policy/ethics/index.html>); the author should secure written confirmation (via letter or email) from the respective ACS journal editor(s) to avoid potential conflicts with journal prior publication*/embargo policies. Appropriate citation of the Published Work must be made. If the thesis or dissertation to be published is in electronic format, a direct link to the Published Work must also be included using the ACS Articles on Request author-directed link – see <http://pubs.acs.org/page/policy/articlesonrequest/index.html>

* Prior publication policies of ACS journals are posted on the ACS website at <http://pubs.acs.org/page/policy/prior/index.html>

If your paper has **not** yet been published by ACS, please print the following credit line on the first page of your article: "Reproduced (or 'Reproduced in part') with permission from [JOURNAL NAME], in press (or 'submitted for publication'). Unpublished work copyright [CURRENT YEAR] American Chemical Society." Include appropriate information.

If your paper has already been published by ACS and you want to include the text or portions of the text in your thesis/dissertation, please print the ACS copyright credit line on the first page of your article: "Reproduced (or 'Reproduced in part') with permission from [FULL REFERENCE CITATION.] Copyright [YEAR] American Chemical Society." Include appropriate information.

Submission to a Dissertation Distributor: If you plan to submit your thesis to UMI or to another dissertation distributor, you should not include the unpublished ACS paper in your thesis if the thesis will be disseminated electronically, until ACS has published your paper. After publication of the paper by ACS, you may release the entire thesis (**not the individual ACS article by itself**) for electronic dissemination through the distributor; ACS's copyright credit line should be printed on the first page of the ACS paper.

Appendix B: Author Permission Letters

Andrew Rasmussen
Utah State University
0300 Old Main Hill
Logan, UT 84322-0300
(801)675-6877

Dr. Karamatullah Danyal
Department of Chemistry and Biochemistry
Utah State University
Logan, Utah 84322

Dear Karamatullah Danyal,

I am currently preparing my thesis and would like your permission to include the following article of which you are a coauthor, as a chapter. I will include an acknowledgment to the article on the first page of the chapter. Please note that USU sends dissertations to Bell and Howell Dissertation services to be made available for reproduction.

Please indicate your approval for this request by signing in the space provided.

If you have any questions, please contact me.

Sincerely,

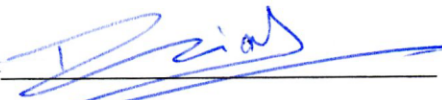
Andrew Rasmussen

I hereby give permission to Andrew Rasmussen to include the following article, of which I am a coauthor, in his thesis.

Danyal, K.; Rasmussen, A. J.; Keable, S. M.; Inglet, B. S.; Shaw, S.; Zadvornyy, O. A.; Duval, S.; Dean, D. R.; Raugei, S.; Peters, J. W.; Seefeldt, L. C. *Biochemistry* **2015**, *54* (15), 2456.

Signed

Date


11/23/2015

Andrew Rasmussen
Utah State University
0300 Old Main Hill
Logan, UT 84322-0300
(801)675-6877

Dr. Boyd S. Inglet
Department of Chemistry and Biochemistry
Utah State University
Logan, Utah 84322

Dear Boyd S. Inglet,
I am currently preparing my thesis and would like your permission to include the following article of which you are a coauthor, as a chapter. I will include an acknowledgment to the article on the first page of the chapter. Please note that USU sends dissertations to Bell and Howell Dissertation services to be made available for reproduction.

Please indicate your approval for this request by signing in the space provided.

If you have any questions, please contact me.

Sincerely,

Andrew Rasmussen

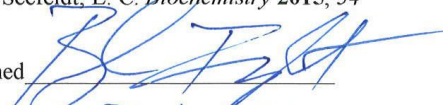
I hereby give permission to Andrew Rasmussen to include the following article, of which I am a coauthor, in his thesis.

Fe Protein-Independent Substrate Reduction by Nitrogenase MoFe Protein Variants

Danyal, K.; Rasmussen, A. J.; Keable, S. M.; Inglet, B. S.; Shaw, S.; Zadvornyy, O. A.; Duval, S.; Dean, D. R.; Raugei, S.; Peters, J. W.; Seefeldt, L. C. *Biochemistry* **2015**, *54* (15), 2456.

Signed

Date



24 Nov 2015

Andrew Rasmussen
Utah State University
0300 Old Main Hill
Logan, UT 84322-0300
(801)675-6877

Dr. John Peters
Department of Chemistry and Biochemistry
Montana State University
Bozeman, Montana 59717

Dear John Peters,

I am currently preparing my thesis and would like your permission to include the following article of which you are a coauthor, as a chapter. I will include an acknowledgment to the article on the first page of the chapter. Please note that USU sends dissertations to Bell and Howell Dissertation services to be made available for reproduction.

Please indicate your approval for this request by signing in the space provided.

If you have any questions, please contact me.

Sincerely,


Andrew Rasmussen

I hereby give permission to Andrew Rasmussen to include the following article, of which I am a coauthor, in his thesis.

Danyal, K.; Rasmussen, A. J.; Keable, S. M.; Inglet, B. S.; Shaw, S.; Zadvornyy, O. A.; Duval, S.; Dean, D. R.; Raugei, S.; Peters, J. W.; Seefeldt, L. C. *Biochemistry* **2015**, *54* (15), 2456.

Signed

Date


11/16/15

Andrew Rasmussen
Utah State University
0300 Old Main Hill
Logan, UT 84322-0300
(801)675-6877

Dr. Dennis R. Dean
Department of Biochemistry
Virginia Tech University, Blacksburg, Virginia 24061

Dear Dennis Dean,

I am currently preparing my thesis and would like your permission to include the following article of which you are a coauthor, as a chapter. I will include an acknowledgment to the article on the first page of the chapter. Please note that USU sends dissertations to Bell and Howell Dissertation services to be made available for reproduction.

Please indicate your approval for this request by signing in the space provided.

If you have any questions, please contact me.

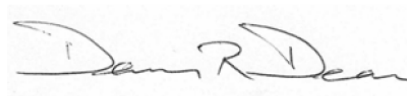
Sincerely,

Andrew Rasmussen

I hereby give permission to Andrew Rasmussen to include the following article, of which I am a coauthor, in his thesis.

Danyal, K.; Rasmussen, A. J.; Keable, S. M.; Inglet, B. S.; Shaw, S.; Zadvornyy, O. A.; Duval, S.; Dean, D. R.; Raugei, S.; Peters, J. W.; Seefeldt, L. C. *Biochemistry* **2015**, *54* (15), 2456.

Signed



Date December 07/2015

Andrew Rasmussen
Utah State University
0300 Old Main Hill
Logan, UT 84322-0300
(801)675-6877

Dr. Oleg A. Zadvornyy
Department of Chemistry and Biochemistry
Montana State University
Bozeman, Montana 59717

Dear Oleg A. Zadvornyy,

I am currently preparing my thesis and would like your permission to include the following article of which you are a coauthor, as a chapter. I will include an acknowledgment to the article on the first page of the chapter. Please note that USU sends dissertations to Bell and Howell Dissertation services to be made available for reproduction.

Please indicate your approval for this request by signing in the space provided.

If you have any questions, please contact me.

Sincerely,

Andrew Rasmussen

I hereby give permission to Andrew Rasmussen to include the following article, of which I am a coauthor, in his thesis.

Danyal, K.; Rasmussen, A. J.; Keable, S. M.; Inglet, B. S.; Shaw, S.; Zadvornyy, O. A.; Duval, S.; Dean, D. R.; Raugei, S.; Peters, J. W.; Seefeldt, L. C. *Biochemistry* **2015**, *54* (15), 2456.

Signed Zadvornyy
Date 11/17/15

Andrew Rasmussen
Utah State University
0300 Old Main Hill
Logan, UT 84322-0300
(801)675-6877

Dr. Simone Raugei
Center for Molecular Electrocatalysis
Pacific Northwest National Laboratory One Shields Avenue
P.O. Box 999, K2-57
Richland, Washington 99352

Dear Simone Raugei,

I am currently preparing my thesis and would like your permission to include the following article of which you are a coauthor, as a chapter. I will include an acknowledgment to the article on the first page of the chapter. Please note that USU sends dissertations to Bell and Howell Dissertation services to be made available for reproduction.

Please indicate your approval for this request by signing in the space provided.

If you have any questions, please contact me.

Sincerely,

Andrew Rasmussen

I hereby give permission to Andrew Rasmussen to include the following article, of which I am a coauthor, in his thesis.

Danyal, K.; Rasmussen, A. J.; Keable, S. M.; Inglet, B. S.; Shaw, S.; Zadvornyy, O. A.; Duval, S.; Dean, D. R.; Raugei, S.; Peters, J. W.; Seefeldt, L. C. *Biochemistry* **2015**, *54* (15), 2456.

Signed Simone Raugei

Date 12/07/2015

Andrew Rasmussen
Utah State University
Old Main Hill
84322-0300

0300
Logan, UT
(801)675-6877

Stephen Keable
Department of Chemistry and Biochemistry
Montana State University
Bozeman, Montana 59717

Dear Stephen Keable,

I am currently preparing my thesis and would like your permission to include the following article of which you are a coauthor, as a chapter. I will include an acknowledgment to the article on the first page of the chapter. Please note that USU sends dissertations to Bell and Howell Dissertation services to be made available for reproduction.

Please indicate your approval for this request by signing in the space provided.

If you have any questions, please contact me.

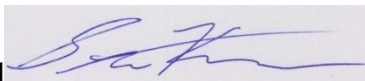
Sincerely,

Andrew Rasmussen

I hereby give permission to Andrew Rasmussen to include the following article, of which I am a coauthor, in his thesis.

Danyal, K.; Rasmussen, A. J.; Keable, S. M.; Inglet, B. S.; Shaw, S.; Zadvornyy, O. A.; Duval, S.; Dean, D. R.; Raugei, S.; Peters, J. W.; Seefeldt, L. C. *Biochemistry* **2015**, *54* (15), 2456.

Signed



Date 11/16/15 _____

Andrew Rasmussen
Utah State University
Old Main Hill
84322-0300

0300
Logan, UT
(801)675-6877

Dr. Simon Duval
Department of Chemistry and Biochemistry
Utah State University
Logan, Utah 84322

Dear Simon Duval,

I am currently preparing my thesis and would like your permission to include the following article of which you are a coauthor, as a chapter. I will include an acknowledgment to the article on the first page of the chapter. Please note that USU sends dissertations to Bell and Howell Dissertation services to be made available for reproduction.

Please indicate your approval for this request by signing in the space provided.

If you have any questions, please contact me.

Sincerely,

Andrew Rasmussen

I hereby give permission to Andrew Rasmussen to include the following article, of which I am a coauthor, in his thesis.

Danyal, K.; Rasmussen, A. J.; Keable, S. M.; Inglet, B. S.; Shaw, S.; Zadvornyy, O. A.; Duval, S.; Dean, D. R.; Raugei, S.; Peters, J. W.; Seefeldt, L. C. *Biochemistry* **2015**, *54* (15), 2456.

Signed _____

Date: 11/17/2015

Andrew Rasmussen
Utah State University
0300 Old Main Hill
Logan, UT 84322-0300
(801)675-6877

Dr. Sudipta Shaw
Department of Chemistry and Biochemistry
Utah State University
Logan, Utah 84322

Dear Sudipta Shaw,

I am currently preparing my thesis and would like your permission to include the following article of which you are a coauthor, as a chapter. I will include an acknowledgment to the article on the first page of the chapter. Please note that USU sends dissertations to Bell and Howell Dissertation services to be made available for reproduction.

Please indicate your approval for this request by signing in the space provided.

If you have any questions, please contact me.

Sincerely,

Andrew Rasmussen

I hereby give permission to Andrew Rasmussen to include the following article, of which I am a coauthor, in his thesis.

Danyal, K.; Rasmussen, A. J.; Keable, S. M.; Inglet, B. S.; Shaw, S.; Zadvornyy, O. A.; Duval, S.; Dean, D. R.; Raugei, S.; Peters, J. W.; Seefeldt, L. C. *Biochemistry* **2015**, *54* (15), 2456.

Signed Sudipta Shaw
Date 12/07/2015